




Descending dopaminergic pathway facilitates itch signal processing via activating spinal GRPR⁺ neurons

Zhi-Jun Zhang^{1,2,*†} , Han-Yu Shao^{2,†}, Chuan Liu^{2,†}, Hao-Lin Song^{2,†}, Xiao-Bo Wu¹ , De-Li Cao¹, Meixuan Zhu³, Yuan-Yuan Fu¹, Juan Wang² & Yong-Jing Gao^{1,**} 

Abstract

A11 dopaminergic neurons regulate somatosensory transduction by projecting from the diencephalon to the spinal cord, but the function of this descending projection in itch remained elusive. Here, we report that dopaminergic projection neurons from the A11 nucleus to the spinal dorsal horn (dopaminergic^{A11-SDH}) are activated by pruritogens. Inhibition of these neurons alleviates itch-induced scratching behaviors. Furthermore, chemogenetic inhibition of spinal dopamine receptor D1-expressing (DRD1⁺) neurons decreases acute or chronic itch-induced scratching. Mechanistically, spinal DRD1⁺ neurons are excitatory and mostly co-localize with gastrin-releasing peptide (GRP), an endogenous neuropeptide for itch. In addition, DRD1⁺ neurons form synapses with GRP receptor-expressing (GRPR⁺) neurons and activate these neurons via AMPA receptor (AMPA). Finally, spontaneous itch and enhanced acute itch induced by activating spinal DRD1⁺ neurons are relieved by antagonists against AMPAR and GRPR. Thus, the descending dopaminergic pathway facilitates spinal itch transmission via activating DRD1⁺ neurons and releasing glutamate and GRP, which directly augments GRPR signaling. Interruption of this descending pathway may be used to treat chronic itch.

Keywords A11; dopamine; DRD1; GRP; itch

Subject Category Neuroscience

DOI 10.15252/embr.202256098 | Received 6 September 2022 | Revised 10 July 2023 | Accepted 14 July 2023 | Published online 31 July 2023

EMBO Reports (2023) 24: e56098

Introduction

Itch is a unique and conserved sensation across mammalian species that arouses a desire to scratch. However, chronic itch often results in serious skin damage and dramatic loss in the quality of life (Dong

& Dong, 2018; Mack & Kim, 2018). The spinal dorsal horn (SDH) is an important area in relaying itch information from peripheral tissue to supraspinal areas (Ikoma *et al.*, 2006; Koch *et al.*, 2018). In addition, local neural circuits in the SDH play a pivotal role in transmitting and gating chemical and mechanical itch (Dong & Dong, 2018; Duan *et al.*, 2018). Particularly, spinally restricted ablation of gastrin-releasing peptide-expressing (GRP⁺) or GRP receptor-expressing (GRPR⁺) neurons reduces itch-related behaviors to different pruritogens, while their chemogenetic excitation elicits itch-like behaviors and facilitates responses to several pruritogens (Sun & Chen, 2007; Sun *et al.*, 2009; Albisetti *et al.*, 2019; Pagani *et al.*, 2019). Furthermore, GRPR⁺ neurons are activated by natriuretic peptide receptor A-expressing (NPRA⁺) neurons, NPRC⁺ neurons, and neuromedin B receptor-expressing (NMBR⁺) neurons to mediate chemical itch (Mishra & Hoon, 2013; Zhao *et al.*, 2014b; Meng *et al.*, 2021). Meanwhile, spinal inhibitory neurons expressing galanin or dynorphin directly inhibit GRPR⁺ neurons to alleviate chemical itch (Kardon *et al.*, 2014; Huang *et al.*, 2018), indicating that GRPR⁺ neurons serve as a cardinal hub for itch processing in the SDH.

Spinal itch transmission is also modulated by the descending pathways from supraspinal areas, such as primary somatosensory cortex, periaqueductal gray (PAG), rostral ventromedial medulla (RVM), and locus coeruleus (LC; Liu *et al.*, 2009; Zhao *et al.*, 2014a; Gao *et al.*, 2019; Koga *et al.*, 2020; Wu *et al.*, 2021). Among them, serotonergic neurons in the RVM stimulate spinal GRPR⁺ neurons and facilitate itch processing via co-activating 5-HT1A and GRPR (Zhao *et al.*, 2014a). RVM neurons also form inhibitory synapses with spinal GRPR⁺ neurons to suppress itch transmission (Liu *et al.*, 2019a). Dopamine, as one of the monoamine transmitters, is widely distributed in the brain reward system (Hu, 2016; Luo & Huang, 2016; Carta *et al.*, 2019), which also plays a role in supraspinal modulation of itch. For example, dopaminergic neurons in the ventral tegmental area (VTA) mediate reward for scratch-induced relief of itch (Su *et al.*, 2019). In addition, VTA dopaminergic

¹ Institute of Pain Medicine and Special Environmental Medicine, Co-Innovation Center of Neuroregeneration, Nantong University, Jiangsu, China

² Department of Human Anatomy, School of Medicine, Nantong University, Jiangsu, China

³ University of North Carolina at Chapel Hill, Chapel Hill, NC, USA

*Corresponding author. Tel: +86 513 55003374; E-mail: gaoyongjing@ntu.edu.cn

**Corresponding author. Tel: +86 513 85051717; E-mail: zhzhj@ntu.edu.cn

[†]These authors contributed equally to this work

neurons projecting to the nucleus accumbens modulate itch processing in the brain (Yuan *et al.*, 2018; Liang *et al.*, 2022). In the diencephalon A11, dopaminergic neurons project to the spinal cord and provide the primary source of spinal dopamine (Qu *et al.*, 2006; Koblinger *et al.*, 2014; Ozawa *et al.*, 2017), whether and how this descending dopaminergic pathway contributes to itch remains largely unknown.

In the present study, we found that projection neurons from the A11 to the SDH (dopaminergic^{A11-SDH}) were activated by pruritogens. Dopaminergic^{A11-SDH} neurons facilitate spinal itch processing via dopamine D1 receptor (DRD1). In addition, a majority of DRD1⁺ neurons express GRP and form a monosynaptic excitatory connection with GRPR⁺ neurons. Thus, we demonstrated that dopaminergic^{A11-SDH} neurons contribute to the facilitation of spinal itch transmission via a neuronal pathway formed by DRD1⁺ neurons and GRPR⁺ neurons.

Results

Dopaminergic^{A11-SDH} neurons facilitate compound 48/80 (C48/80)- or chloroquine (CQ)-induced itch

First, we examined the spatial distribution of A11 dopaminergic neurons projecting to the cervical SDH. FluoroGold (FG) retrograde tracer was injected into the SDH between C4 and C6 (Appendix Fig S1A). The brain sections containing the A11 were stained with TH (tyrosine hydroxylase, a marker for dopaminergic neurons) antibodies. It showed that FG⁺ neurons were bilaterally distributed and preferred to the ipsilateral side of the A11. In addition, FG⁺TH⁺ neurons were distributed between Bregma -2.3 and -2.9 mm, with the peak at Bregma -2.54 mm (Appendix Fig S1B–D).

We then used the Cre/Loxp and Flpo/FRT strategies to label dopaminergic^{A11-SDH} neurons and examine the correlation between GCaMP6s fluorescent signals and scratching trains (Fig 1A). First, the retrograde and Cre-dependent AAV (AAV-retro-DIO-Flpo) was injected into cervical SDH of TH-cre mice to cause Flpo expression in brain TH⁺ neurons. One week later, the Flpo-dependent AAV (AAV-fDIO-GCaMP6s or EYFP) was injected into the A11 to cause GCaMP6s or EYFP expression in Flpo⁺ neurons. About 95% of GCaMP6s⁺ neurons were co-localized with TH, and 70% of TH⁺ neurons were co-localized with GCaMP6s in the A11 (Fig 1B). Furthermore, GCaMP6s fluorescent signals were elevated during scratching induced by intra-nape injection of C48/80 (Fig 1C–E) or CQ (Fig 1F–H). To test whether these signals are induced by mechanical nociception elicited by scratching, we used Elizabethan collar to protect mice from scratching the nape skin (Fig EV1A). We found that GCaMP6s fluorescent signals were still elevated when the mice attempted to scratch (Fig EV1B–G). In contrast, the movement of removing sticky tape from the ear of naive mice did not increase GCaMP6s fluorescent signals (Fig EV1H–K). These data suggested that dopaminergic^{A11-SDH} neurons were activated by acute itch.

To investigate the role of A11 dopaminergic neurons in itch processing, 6-hydroxydopamine (6-OHDA, the neurotoxin to dopaminergic neurons; Kim *et al.*, 2011) was bilaterally injected into the A11, which caused a large loss of dopaminergic neurons 14 days after injection (Fig EV2A–C). Accordingly, C48/80- and CQ-induced

scratches were decreased (Fig EV2D), with the motor function intact (Fig EV2E and F), indicating the involvement of A11 dopaminergic neurons in acute itch. We further tested the role of dopaminergic^{A11-SDH} neurons in itch by chemogenetic manipulations (Fig 1I). After the AAV-retro-DIO-Flpo and AAV-fDIO-mCherry (mCherry) were, respectively, injected into the SDH and the A11 of TH-Cre mice (Appendix Fig S2A), mCherry⁺ neurons were spatially restricted in the A11 (Appendix Fig S2B and C), and the axonal terminals of mCherry-labeled dopaminergic^{A11-SDH} neurons were shown in the bilateral dorsal horn and ventral horn (Appendix Fig S2D). After the AAV-retro-DIO-Flpo and AAV-fDIO-hM4Di-mCherry (hM4Di) or AAV-fDIO-hM3Dq-mCherry (hM3Dq) were injected (Fig 1I), perfusion of clozapine-N-oxide (CNO) decreased or increased the excitability of dopaminergic^{A11-SDH} neurons expressing hM4Di or hM3Dq, respectively (Appendix Fig S2E–G). Furthermore, intraperitoneal (i.p.) injection of CNO decreased itchy scratching induced by C48/80 or CQ in the hM4Di group (Fig 1J), and increased scratching in the hM3Dq group (Fig 1K). However, neither chemogenetic activation nor optogenetic activation of dopaminergic^{A11-SDH} neurons induced spontaneous scratching behaviors (Fig EV3A–E). In addition, chemogenetic activation or inhibition of dopaminergic^{A11-SDH} neurons did not affect mechanical itch induced by light punctate stimuli (0.008, 0.04, and 0.07 g), mechanical threshold for von Frey filament test, thermal response latencies for Hargreaves test and hot/cold plate test, or motor function for Rota-rod and open-field test (Fig EV3F–L). These results suggest that dopaminergic^{A11-SDH} neurons facilitate acute itch processing.

We then examined c-Fos expression in the spinal cord after chemogenetic manipulation of dopaminergic^{A11-SDH} neurons. Intradermal injection of C48/80 or CQ combining i.p. injection of saline markedly increased c-Fos expression in the SDH of TH-cre mice injected with Cre-dependent AAVs expressing mCherry, hM4Di, or hM3Dq in the A11 (Appendix Fig S3A–F). In contrast, after i.p. injection of CNO, the increased c-Fos expression by C48/80 or CQ was reduced in the hM4Di group but was further increased in the hM3Dq group (Appendix Fig S3G–J), confirming that dopaminergic^{A11-SDH} neurons regulate acute itch at the spinal cord level.

Dopaminergic^{A11-SDH} neurons facilitate diphenylcyclopropenone (DCP)-induced itch

Topically applying DCP to the nape skin caused persistent scratching behaviors (Appendix Fig S4A and B). The fiber photometry recording showed that GCaMP6s fluorescent signals in dopaminergic^{A11-SDH} neurons were increased by DCP-induced itch (Fig 2A–D). Furthermore, DCP-induced itch was attenuated after bilateral A11 dopaminergic neuron ablation by 6-OHDA (Appendix Fig S4C). In addition, chemogenetic inhibition of dopaminergic^{A11-SDH} neurons expressing hM4Di decreased DCP-induced scratching behaviors (Fig 2E and F), and chemogenetic activation of these neurons expressing hM3Dq enhanced scratching behaviors (Fig 2E and G). Moreover, inhibition or activation of dopaminergic^{A11-SDH} neurons, respectively, decreased or increased spinal c-Fos⁺ neurons induced by DCP (Appendix Fig S4D–G). These results indicate that dopaminergic^{A11-SDH} neurons also play an important role in facilitating chronic itch processing in the spinal cord.

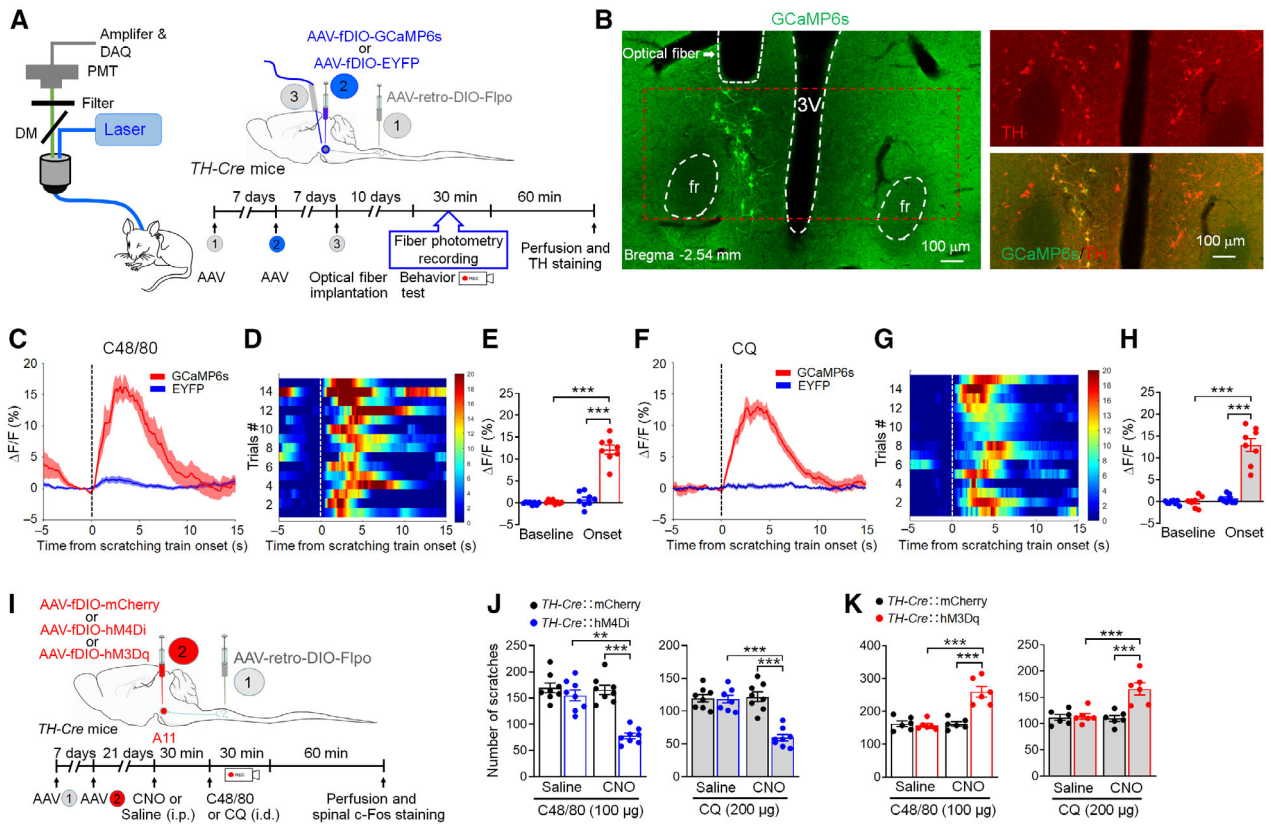


Figure 1. Dopaminergic^{A11-SDH} neurons contribute to C48/80- and CQ-induced acute itch.

- A Schematic drawing shows the fiber photometry recording system (left panel), viral strategy, and the timeline of the experimental setup for GCaMP6s or EYFP expression in dopaminergic^{A11-SDH} neurons (right panel).
- B Representative images show the optical fiber implantation, the expression of GCaMP6s, and the staining of TH in the A11. Right panel images were taken from the red frame in the left panel. 3 V, third ventricle; fr, fasciculus retroflexus. Scale bar, 100 μ m.
- C–E Average fluorescence signals aligned to the onset of scratching trains across the GCaMP6s group (red line) and EYFP group (blue line) in C48/80 model (C). Heatmap illustration of fluorescence changes during each corresponding scratching train in GCaMP6s group. $n = 8$ mice/group. Two trials for each are shown except for one mouse where one trial was performed (D). Quantification of average fluorescence signals in GCaMP6s and EYFP groups during the baseline and scratching train onset periods (E). *** $P < 0.001$. Two-way ANOVA followed by Bonferroni's test. $n = 8$ mice/group.
- F–H Average fluorescence signals aligned to the onset of scratching trains across the GCaMP6s group (red line) and EYFP group (blue line) in CQ model (F). Heatmap illustration of fluorescence changes during each corresponding scratching train in GCaMP6s group. $n = 8$ mice/group. Two trials for each are shown except for one mouse where one trial was performed (G). Quantification of average fluorescence signals in GCaMP6s and EYFP groups during the baseline and scratching train onset periods (H). *** $P < 0.001$. Two-way ANOVA followed by Bonferroni's test. $n = 8$ mice/group.
- I Chemogenetic strategy to label dopaminergic^{A11-SDH} neurons (upper panel) and the timeline of the experimental setup for acute itch in *TH-Cre* mice (lower panel).
- J, K Effect of chemogenetic inhibition (J) or activation (K) of dopaminergic^{A11-SDH} neurons on scratching behaviors in response to C48/80 (left) and CQ (right) stimuli. ** $P < 0.01$, *** $P < 0.001$. Two-way ANOVA followed by Bonferroni's test. $n = 6$ –8 mice/group.

Data information: Bars represent mean values. Error bars indicate the SEM.

Source data are available online for this figure.

Spinal dopamine receptor D1 contributes to acute and chronic itch

Dopamine affects intracellular signaling transduction pathways through D1-like receptors (comprising DRD1 and DRD5) and D2-like receptors (comprising DRD2, DRD3, and DRD4; Beaulieu & Gainetdinov, 2011). To examine whether spinal D1-like and/or D2-like receptors are involved in acute itch, we intrathecally (i.t.) injected SCH23390, a D1-like receptor antagonist (Tao et al, 2017), or sulpiride, a D2-like receptor antagonist (Janssen et al, 2015), before C48/80 or CQ injection. SCH23390 at the concentrations of 20 and 200 μ M (10 μ l) reduced the scratches induced by C48/80 or CQ.

However, the same dose of sulpiride did not show such effects (Fig 3A). In addition, both SCH23390 and sulpiride individually injected at either 20 or 200 μ M did not affect the motor function (Appendix Fig S5A and B). Furthermore, SCH23390 but not sulpiride decreased the number of spinal c-Fos⁺ neurons induced by C48/80 or CQ (Appendix Fig S5C and D). Similarly, SCH23390, but not sulpiride, reduced DCP-induced scratching behaviors (Fig 3B and C) and decreased the number of c-Fos⁺ neurons in cervical SDH of DCP-treated mice (Appendix Fig S5E and F). Interestingly, DCP treatment for 6 days induced an increase in *Drd1* mRNA level in the spinal cord (Fig 3D). These data indicate that spinal D1-like receptors are involved in itch transmission in the spinal cord.

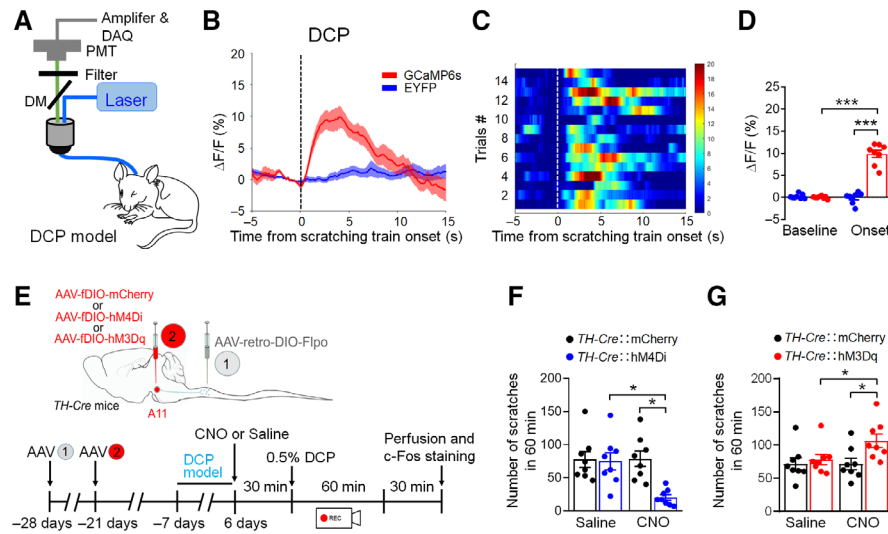


Figure 2. Dopaminergic^{A11-SDH} neurons contribute to DCP-induced chronic itch.

- A** Schematic drawing shows the fiber photometry recording system in DCP model.
- B–D** Average fluorescence signals aligned to the onset of scratching trains across the GCaMP6s group (red line) and EYFP group (blue line) in DCP model (B). Heatmap illustration of fluorescence change during each corresponding scratching train in GCaMP6s group. $n = 8$ mice/group. Two trials for each are shown except for one mouse where one trial was performed (C). Quantification of average fluorescence signals in GCaMP6s and EYFP groups during the baseline and scratching train onset periods (D). *** $P < 0.001$. Two-way ANOVA followed by Bonferroni's test. $n = 8$ mice/group.
- E** Strategy for chemogenetic manipulation of dopaminergic A_{11} -SDH neurons (upper panel) and the timeline of the experimental setup for DCP-induced chronic itch in *TH-Cre* mice (lower panel).
- F, G** Effect of chemogenetic inhibition (F) or activation (G) of dopaminergic A_{11} -SDH neurons on DCP-induced scratching. * $P < 0.05$. Two-way ANOVA followed by Bonferroni's test. $n = 8$ mice/group.

Data information: Bars represent mean values. Error bars indicate the SEM. Source data are available online for this figure.

We then asked if the D1-like receptor agonist SKF38393 was sufficient to induce itch. I.t. injection of SKF38393 (200 μ M) alone did not induce scratching behaviors. However, SKF38393 enhanced scratches induced by C48/80 or CQ at different doses (Fig 3E), suggesting that the activation of D1-like receptors is not sufficient to induce spontaneous itch but enhances pruritogens-induced acute itch.

We next investigated the effect of SKF38393 on the neuronal excitability of spinal DRD1⁺ neurons using electrophysiological recording (Fig 3F). Whole-cell patch-clamp recordings revealed that SKF38393 alone did not induce the spike firing of spinal DRD1⁺ neurons, but increased the firing frequency (Fig 3G and H). In addition, SKF38393 caused a remarkable shift to the depolarizing direction in resting membrane potential compared with the vehicle (Fig 3I). Other parameters such as threshold, fast AHP, maximal decaying slope, half-width, rheobase, and slower rising rate were comparable between SKF38393 and vehicle groups (Appendix Table S1). Furthermore, we stimulated spinal terminals of dopaminergic A_{11} -SDH neurons labeled with hChR2, and then recorded the firing frequency of spinal DRD1⁺ neurons in *TH-Cre*^{+/−};*Drd1-tdTomato*^{+/−} mice (Fig 3J). Bursting activation of dopaminergic A_{11} -SDH neurons induced a delayed (24.5 ± 5.5 s, $n = 8$ neurons) increase in the firing frequency of spinal DRD1⁺ neurons, but did not evoke action potentials or change the firing pattern (Fig 3K and L). These data suggest that dopaminergic descending pathway induces increased neuronal excitability of spinal DRD1⁺ neurons via DA under itch conditions.

Spinal DRD1⁺ neurons contribute to acute and chronic itch

We further checked if DRD1⁺ neurons in the spinal cord are involved in itch transmission. We used AAV-DIO-taCasp3 to specifically ablate DRD1⁺ neurons in the cervical SDH of *Drd1-Cre* mice (Fig 4A). After injection of AAV-DIO-mCherry into the SDH of *Drd1-Cre* mice, mCherry⁺ neurons were mainly distributed in the spinal lamina II (Appendix Fig S6A). AAV-DIO-taCasp3 injection eliminated most of mCherry⁺ neurons and reduced *Drd1* mRNA level in the SDH of *Drd1-Cre* mice (Appendix Fig S6B and C). The ablation of DRD1⁺ neurons in the SDH markedly decreased the number of scratches evoked by C48/80, CQ, or DCP (Fig 4B and C).

We further tested the role of spinal DRD1⁺ neurons in acute itch using chemogenetic approach. The AAV-DIO-mCherry (mCherry), AAV-DIO-hM4Di-mCherry (hM4Di), or AAV-DIO-hM3Dq-mCherry (hM3Dq) was injected into the cervical SDH of *Drd1-Cre* mice (Fig 4D). Electrophysiological recording confirmed the inhibitory or excitatory effect of CNO on spinal DRD1⁺ neurons in the spinal slices of *Drd1-Cre* mice injected with hM4Di or hM3Dq, respectively (Appendix Fig S6D–F). Inhibition of spinal DRD1⁺ neurons by CNO decreased the scratches evoked by C48/80 or CQ in the hM4Di group (Fig 4E), and activation of spinal DRD1⁺ neurons by CNO increased the scratches evoked by C48/80 or CQ in the hM3Dq group (Fig 4F). Interestingly, activation of spinal DRD1⁺ neurons by CNO resulted in spontaneous scratching behaviors (Fig 4G).

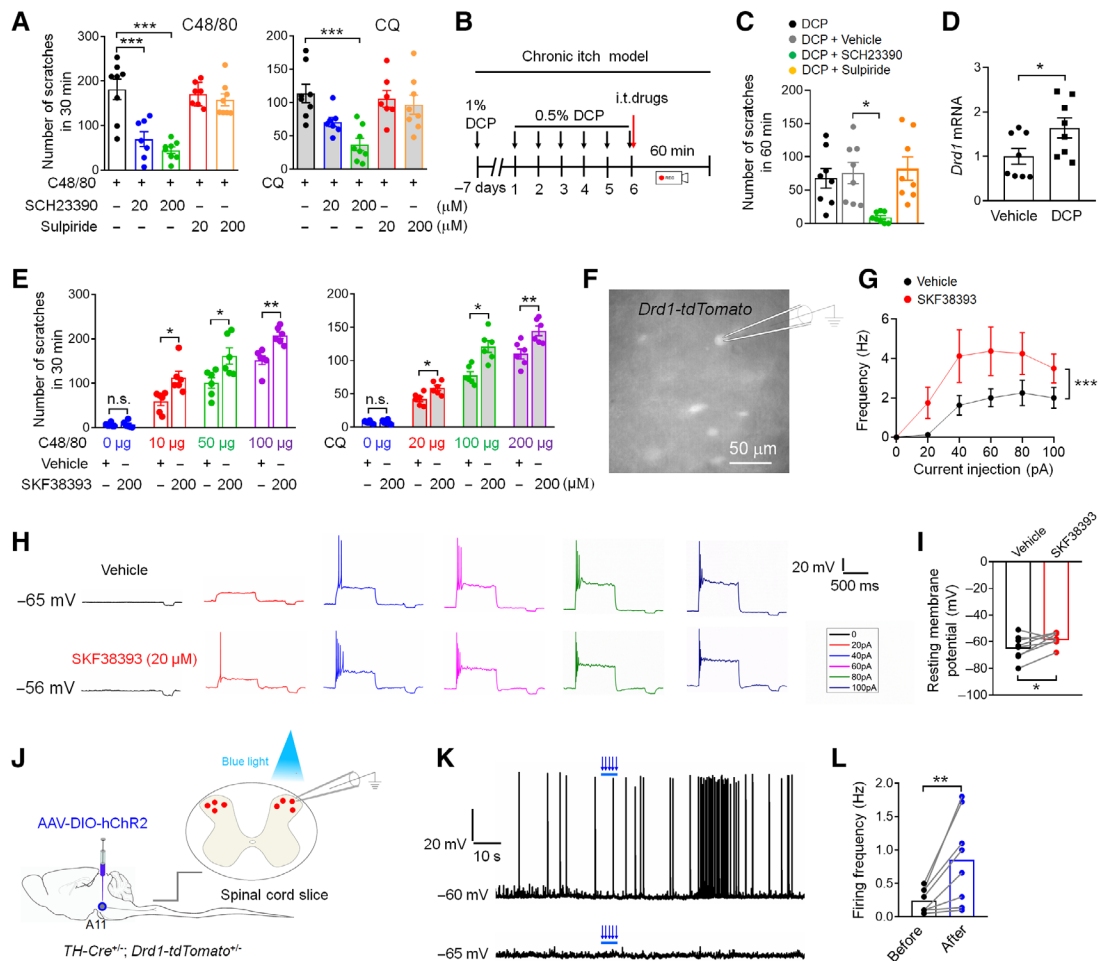


Figure 3. Spinal DRD1 is involved in itch processing and DRD1⁺ neurons' excitability.

- A Effect of SCH23390 and sulpiride on scratching behaviors induced by C48/80 (left) and CQ (right). *** $P < 0.001$. One-way ANOVA followed by Bonferroni's test. $n = 7-8$ mice/group.
- B Timeline of DCP topical treatment, drug administration, and behavioral testing.
- C Effect of SCH23390 and sulpiride on DCP-induced scratching behaviors. * $P < 0.05$. One-way ANOVA followed by Bonferroni's test. $n = 8$ mice/group.
- D The *Drd1* mRNA level in the spinal cord after DCP or vehicle treatment. * $P < 0.05$. Student's *t*-test. $n = 8$ mice/group.
- E Effect of SKF38393 on C48/80- and CQ-induced scratching behaviors. * $P < 0.05$, ** $P < 0.01$. Student's *t*-test. $n = 6$ mice/group.
- F Image shows *Drd1-tdTomato*⁺ neurons and electrophysiological recording. Scale bar, 100 μ m.
- G Statistical curve shows the firing frequency evoked by step current injection into DRD1⁺ neurons that incubated with vehicle or SKF38393. *** $P < 0.001$. Two-way ANOVA. $n = 8$ neurons/group.
- H Representative traces of vehicle- (upper panels) and SKF38393-treated (lower panels) DRD1⁺ neurons in the spinal cord of *Drd1-tdTomato* mice after injection of different currents.
- I Statistical histogram shows the resting membrane potential in DRD1⁺ neurons incubated with vehicle or SKF38393. * $P < 0.05$. Paired Student's *t*-test. $n = 8$ neurons/group.
- J Strategy for stimulating the terminals of dopaminergic^{A11-SDH} neurons by optogenetics in spinal slice and the recording of spikes of DRD1⁺ neurons labeled with tdTomato.
- K Representative traces from one spinal DRD1⁺ neuron show that blue light stimuli did not induce spontaneous firing (holding potential, -65 mV, lower panel) but increased the existing firing of DRD1⁺ neuron (holding potential, -60 mV, upper panel). Arrows indicate blue light stimuli (2–3 mW/cm², 5 pulses, 2 ms duration, 20 Hz, and repeated every 1 s).
- L Histogram shows the change in firing frequency from individual DRD1⁺ neurons after blue light stimuli. ** $P < 0.01$. Paired Student's *t*-test. $n = 8$ neurons/group.

Data information: Bars represent mean values. Error bars indicate the SEM.

Source data are available online for this figure.

We then checked the effect of chemogenetic regulation of spinal DRD1⁺ neurons on DCP-induced itch (Fig 4H). These AAVs were bilaterally injected into the cervical SDH of *Drd1-Cre* mice. Inhibition

of spinal DRD1⁺ neurons by CNO alleviated DCP-induced scratching behaviors in the hM4Di group (Fig 4I). On the contrary, activation of spinal DRD1⁺ neurons by CNO increased DCP-induced scratching

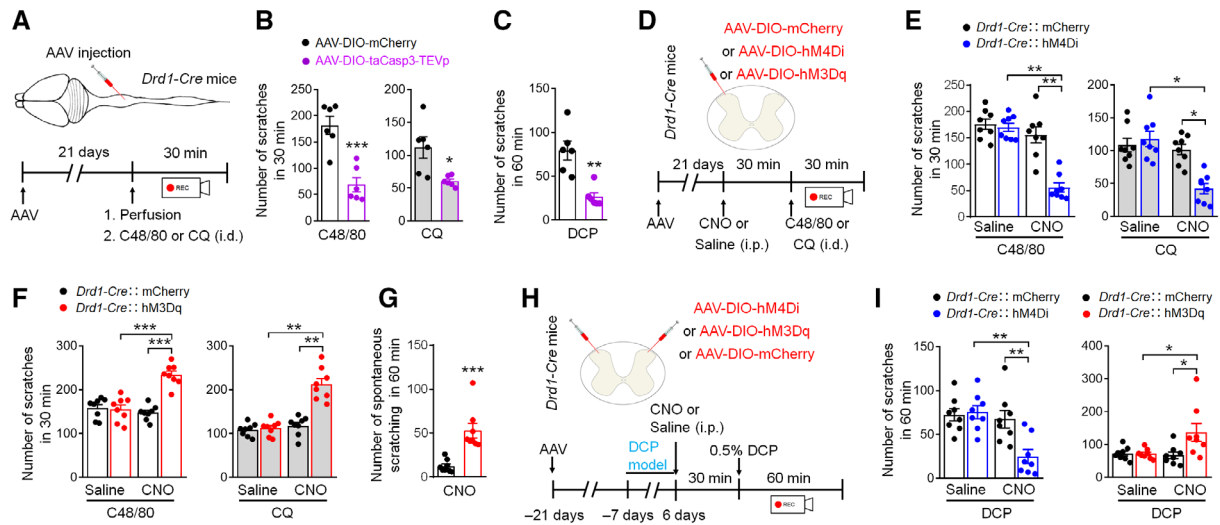


Figure 4. Spinal DRD1⁺ neurons contribute to acute and chronic itch.

- A Schematic drawing shows the AAV injection in the cervical SDH of *Drd1-Cre* mice (upper panel) and the timeline of the experimental setup in *Drd1-Cre* mice (lower panel).
- B Effect of AAV injection on the scratching behaviors induced by C48/80 (left) and CQ (right). * $P < 0.05$, *** $P < 0.001$. Student's *t*-test. $n = 6$ mice/group.
- C Effect of AAV injection on DCP-induced chronic itch behaviors. ** $P < 0.01$. Student's *t*-test. $n = 6$ mice/group.
- D Strategy for the injection of chemogenetic AAVs in *Drd1-cre* mice (upper panel) and the timeline of the experimental setup for the acute itch model (lower panel).
- E, F Effect of chemogenetic inhibition (E) or activation (F) of spinal DRD1⁺ neurons on the scratching behaviors in response to C48/80 and CQ stimuli. * $P < 0.05$, ** $P < 0.01$, *** $P < 0.001$. Two-way ANOVA followed by Bonferroni's test. $n = 8$ mice/group.
- G Effect of chemogenetic activation of spinal DRD1⁺ neurons on spontaneous itch behaviors. *** $P < 0.001$. Student's *t*-test. $n = 8$ mice/group.
- H Strategy for the injection of chemogenetic AAVs in *Drd1-cre* mice (upper panel) and the timeline of the experimental setup for chronic itch model (lower panel).
- I Effect of chemogenetic inhibition (left) or activation (right) of spinal DRD1⁺ neurons on the DCP-induced chronic itch behaviors. * $P < 0.05$, ** $P < 0.01$. Two-way ANOVA followed by Bonferroni's test. $n = 8$ mice/group.

Data information: Bars represent mean values. Error bars indicate the SEM.

Source data are available online for this figure.

behaviors in the hM3Dq group (Fig 4I). These data indicate that spinal DRD1⁺ neurons contribute to acute and chronic itch signal transmission.

To further confirm the role of spinal DRD1⁺ neurons in the facilitation of dopaminergic^{A11-SDH} neurons on itch processing, we injected AAV-retro-Flpo and AAV-DIO-taCasp3-TEVp (or AAV-DIO-mCherry) into cervical spinal dorsal horn of *Drd1-cre* mice and injected AAV-fDIO-hM3Dq-mCherry into the A11 one week later (Fig EV4A). Behavioral tests showed that the increase in C48/80- or CQ-induced scratching by the activation of A11- spinal cord projection neurons was dramatically decreased following the ablation of spinal DRD1⁺ neurons (Fig EV4B). Similarly, the same treatment blocked the enhancement of scratching in DCP-treated mice (Fig EV4C and D), indicating that the facilitation of dopaminergic^{A11-SDH} neurons on acute and chronic itch is dependent on spinal DRD1⁺ neurons.

Spinal DRD1⁺ neurons are excitatory and distributed in the lamina II of SDH

We then examined the distribution of spinal DRD1⁺ neurons using *Drd1-tdTomato* mice. tdTomato-expressing DRD1⁺ cells form a concentrated band in the superficial layer of the dorsal horn (Fig 5A). FISH (fluorescence *in situ* hybridization) staining further showed that 91.4% of tdTomato⁺ cells exhibited detectable *Drd1* mRNA

expression, and 93.8% of DRD1⁺ cells exhibited tdTomato protein expression (Fig 5B–E), indicating that tdTomato marks most of DRD1⁺ cells in the SDH. In contrast, EGFP-expressing DRD2⁺ cells in *Drd2-EGFP* mice were scattered in the SDH and not co-localized with tdTomato signals (Fig 5F–H). Furthermore, tdTomato⁺ cells were largely co-localized with neuronal marker NeuN (Fig 5I), but not co-localized with NK1R (a marker for lamina I, Fig 5J) or CGRP (a marker for the outer layer of lamina II [IIo], Fig 5K). Most of the tdTomato⁺ neurons were intermingled with the terminals of IB4 (a marker for the dorsal inner layer of lamina II [dIII], 44.1%, Fig 5L) and protein kinase C γ (PKC γ , a marker for the ventral inner layer of lamina II [vII], 35.3%, Fig 5M). Therefore, the *Drd1-tdTomato*⁺ neurons are mainly located in lamina III of the SDH.

To further characterize spinal DRD1⁺ neurons, we examined the co-localization of *Drd1* with excitatory or inhibitory neuronal markers. Immunostaining combining FISH showed that most of tdTomato⁺ neurons (96.8%) expressed *slc17a6* mRNA (encoding vGluT2, an excitatory neuronal marker) in the SDH (Fig 5N). Furthermore, double FISH staining with *Drd1* and *slc17a6* probes showed that *Drd1* mRNA was highly co-localized with *slc17a6* mRNA (95.9%, Fig 5O). Immunostaining demonstrated that tdTomato⁺ neurons were rarely co-localized with PAX2 (an inhibitory neuronal marker in the SDH, 3.2%, Fig 5P). To further confirm this result, *Drd1-tdTomato* mice were crossed with *Gad67-EGFP* mice (*Gad67*, an inhibitory neuronal marker). The data showed

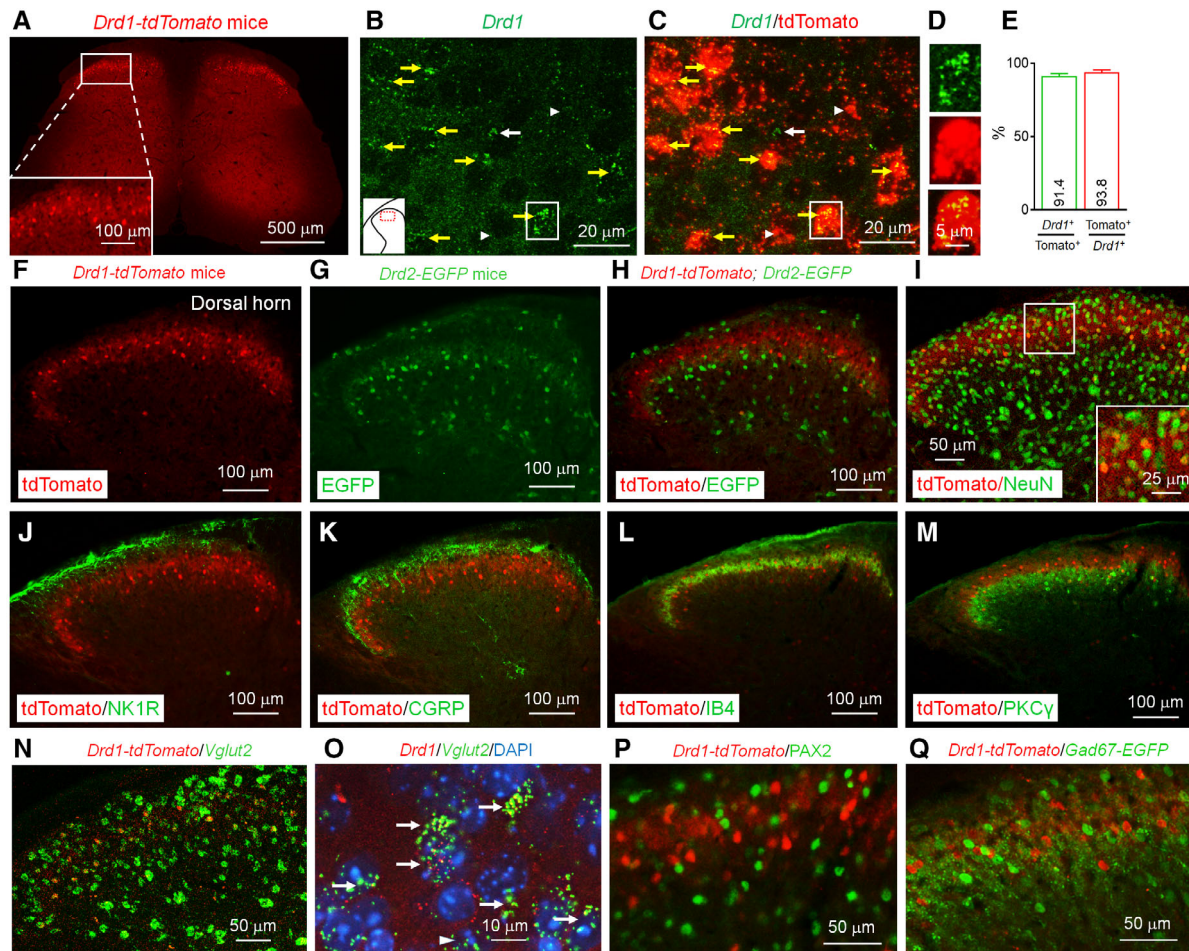


Figure 5. DRD1⁺ neurons are distributed in lamina II of SDH and co-localized with vGluT2.

A tdTomato⁺ neurons were visualized in SDH of *Drd1-tdTomato* mice. Scale bar, 500 μ m.

B–D FISH staining of *Drd1* probe with tdTomato fluorescence. Yellow arrows show double-labeled neurons. White arrow and arrowheads show *Drd1* and tdTomato single-labeled neurons, respectively. The high-magnification images in (D) were taken from the inserted white frames in (B) and (C). Scale bar, 20 μ m in B and C, 5 μ m in D.

E Statistical data show the co-localization percentage of *Drd1* with tdTomato. $n = 3$ mice/group. Error bars indicate the SEM.

F–H Representative images show nonoverlap of tdTomato with EGFP in the SDH of *Drd1-tdTomato;Drd2-EGFP* mice. Scale bar, 100 μ m.

I Representative image shows the co-localization of NeuN with tdTomato. Scale bar, 50 μ m. Inset scale bar, 25 μ m.

J–M Representative images show the co-localization of NK1R (J), CGRP (K), IB4 (L), and PKC γ (M) with tdTomato. Scale bar, 100 μ m.

N Co-localization of tdTomato fluorescence with *vGluT2* probe. Scale bar, 50 μ m.

O FISH double staining of *Drd1* probe with *vGluT2* probe. White arrows and arrowheads show double-labeled neurons and *vGluT2* single-labeled neurons, respectively. Scale bar, 10 μ m.

P Staining of PAX2 in *Drd1-tdTomato* mice. Scale bar, 50 μ m.

Q Fluorescence of tdTomato and EGFP in the SDH of *Drd1-tdTomato;Gad67-EGFP* mice. Scale bar, 50 μ m.

Source data are available online for this figure.

2.1% co-localization between tdTomato and EGFP in their offspring (Fig 5Q). The evidence suggests that spinal DRD1⁺ neurons are excitatory.

Spinal DRD1⁺ neurons form monosynaptic connections with GRPR⁺ neurons

As GRPR⁺ neurons are important in spinal itch transmission, we examined the synaptic connection between spinal DRD1⁺ and GRPR⁺ neurons. The mammalian GFP reconstitution across synaptic

partners (mGRASP) method has been applied to detect the mammalian neuronal synapses with a fluorescence microscope (Choi et al, 2018). When the distance between the pre-mGRASP and post-mGRASP is ~ 20 nm (matching the cleft of a mammalian synapse), the two nonfluorescent split-GFP fragments reconstitute to be fluorescent GFP. We injected AAV-DIO-pre-mGRASP-P2A-mCherry and AAV-fDIO-post-mGRASP into the SDH of *Drd1-Cre^{+/-};Grpr-Flpo^{+/-}* mice to induce the expression of the pre-mGRASP and mCherry in spinal DRD1⁺ neurons and the expression of the post-mGRASP in spinal GRPR⁺ neurons, respectively (Fig 6A and B). Under

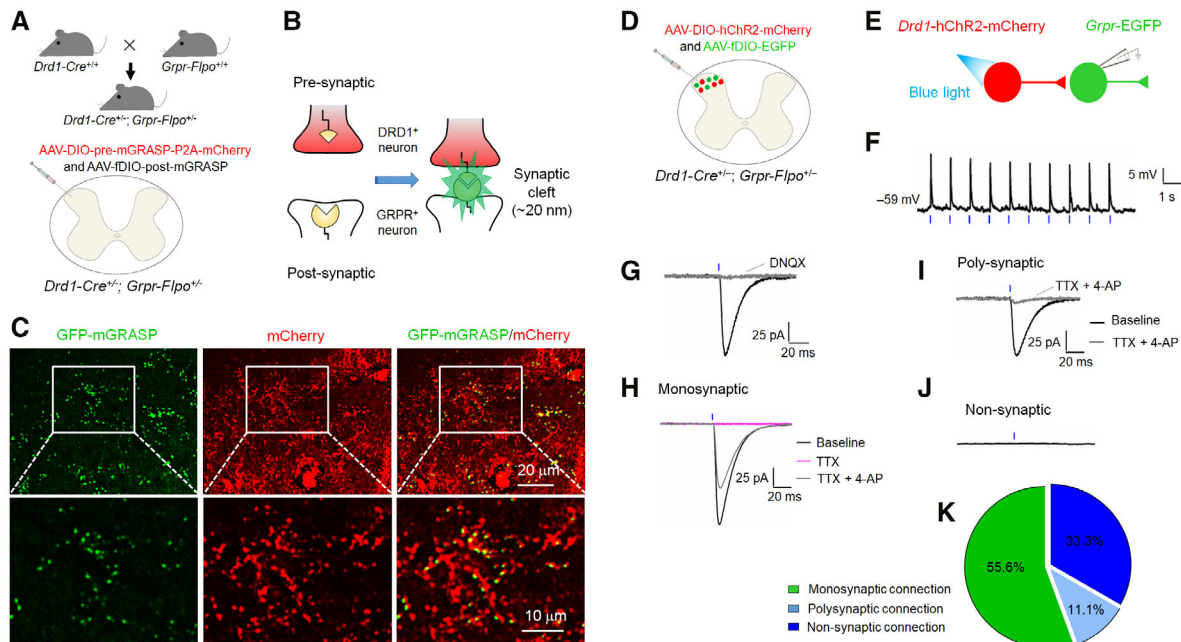


Figure 6. DRD1⁺ neurons form synaptic connections with GRPR⁺ neurons in the SDH.

- A Hybrid strategy to generate the mouse expressing *Drd1-Cre* and *Grpr-Flpo* (upper panel) and the scheme of AAV injection into the SDH to express the pre-mGRASP and mCherry in DRD1⁺ neurons and the post-mGRASP in GRPR⁺ neurons, respectively (lower panel).
- B Schematic illustration of mGRASP technique to exhibit a synapse.
- C Representative images show the reconstitution of pre- and post-mGRASP to form an intact GFP (green), which mapped synaptic connectivity between spinal DRD1⁺ neurons (red, as presynaptic constructs) and GRPR⁺ neurons (upper panels). High-magnification images in the white frames are shown in lower panels. Scale bar, 20 μ m in upper panel and 10 μ m in lower panel.
- D Scheme of AAV injection into the SDH to express the hChR2 and mCherry in DRD1⁺ neurons and the EGFP in GRPR⁺ neurons, respectively.
- E Experimental setup for checking the monosynaptic transmission from the DRD1⁺ neurons to GRPR⁺ neurons in the SDH.
- F A representative trace of the whole-cell current clamp shows the blue light-evoked EPSPs recorded in a GRPR⁺ neuron (470 nm, 2 ms).
- G Representative traces of the whole-cell voltage clamp show the blue light (470 nm, 2 ms)-evoked EPSCs recorded in a GRPR⁺ neuron before (black) and after 20 μ M DNQX perfusion (gray).
- H Representative traces show the effect of TTX alone (purple) and the combined presence of 4-AP (gray) superfusion on the blue light-evoked EPSCs (black) recorded in a GRPR⁺ neuron.
- I Representative traces show the effect of TTX + 4-AP (gray) on the blue light (470 nm, 2 ms)-evoked EPSCs (black) recorded in a GRPR⁺ neuron.
- J A representative trace shows no response of GRPR⁺ neuron to the blue light (470 nm, 2 ms).
- K Pie chart shows the percentage of monosynaptic, polysynaptic, and nonsynaptic connections between DRD1⁺ neurons and GRPR⁺ neurons in the SDH.
- Source data are available online for this figure.

fluorescence microscopy, we captured GFP-labeled punctate synapses formed by spinal DRD1⁺ and GRPR⁺ neurons (Fig 6C). We also observed mCherry-labeled cell bodies and neurites of spinal DRD1⁺ neurons, which represent the presynaptic structure (Fig 6C).

We further checked the functional connection between spinal DRD1⁺ and GRPR⁺ neurons by electrophysiology. We injected AAVs into the SDH of *Drd1-Cre*^{+/-}; *Grpr-Flpo*^{+/-} mice to express hChR2 and EGFP in DRD1⁺ and GRPR⁺ neurons, respectively (Fig 6D). Thus, it allows electrophysiological recording of spinal GRPR⁺ neurons following optogenetic activation of spinal DRD1⁺ neurons (Fig 6E). To begin with, we recorded stable excitatory postsynaptic potentials (EPSPs) upon DRD1⁺ neurons in the spinal slice stimulated by short blue light (470 nm, 2 ms) under current-clamp conditions (Fig 6F). Then, we recorded evoked excitatory postsynaptic currents (EPSCs) in spinal GRPR⁺ neurons upon optogenetic excitation of spinal DRD1⁺ neurons (2 ms, 470 nm blue light) after switching to voltage-clamp mode. Perfusion of the spinal slice with DNQX (a specific and competitive AMPA receptor antagonist,

20 μ M) nearly blocked the recorded EPSCs (Fig 6G). Tetrodotoxin (TTX, 1 μ M) perfusion completely blocked the recorded EPSCs (Fig 6H). Furthermore, 4-AP (4-aminopyridine, a nonselective K⁺ channel blocker, 20 μ M) perfusion partially reversed TTX-blocked EPSCs (Fig 6I). The EPSCs were occasionally missed after the excitation of spinal DRD1⁺ neurons (Fig 6J). The percentage of the above three types of neurons is shown in Fig 6K. These data indicate that most of the synapses between spinal DRD1⁺ and GRPR⁺ neurons are glutamatergic monosynaptic connections.

GRP and glutamate contribute to DRD1-mediated itch transmission

As spinal GRP⁺ neurons are excitatory (Mishra & Hoon, 2013; Albi-setti et al, 2019), we asked whether DRD1 is co-localized with GRP in the SDH. FISH combined with immunofluorescence staining showed that tdTomato signals largely overlapped with *Grp* mRNA in

superficial SDH (Fig 7A). In contrast, tdTomato signals rarely co-localized with *Grpr* mRNA (Fig 7B). The statistical data showed that approximately 77% of tdTomato⁺ neurons contained *Grp* mRNA (Fig 7C). Single-cell RT-PCR further showed that 7 of 10 (70%) tdTomato⁺ neurons expressed *Grp* mRNA (Fig 7D). Behavioral tests showed that i.t. injection of GRP induced scratching behaviors, which was not affected by SCH23390 (Fig 7E), suggesting that DRD1 locates upstream of GRPR signaling. Moreover, ablation of GRPR⁺ neurons by i.t. injection of bombensin saporin blocked chemogenetic activation of DRD1⁺ neurons-induced spontaneous scratching (Fig 7F and G). I.t. injection of DNQX or GRPR blocker RC-3095 also decreased this spontaneous scratching (Fig 7H and I) and relieved

C48/80- or CQ-induced itch. Furthermore, the enhanced C48/80- or CQ-induced itch by chemogenetic activation of DRD1⁺ neurons was attenuated by DNQX and RC-3095 (Fig 7J), confirming the contribution of glutamate and GRP from spinal DRD1⁺ neurons in itch processing.

Discussion

Dopaminergic fibers, along with others such as serotonergic, noradrenergic, and GABAergic fibers, are vital descending pathways projecting to the spinal cord. Previous studies indicated the role of

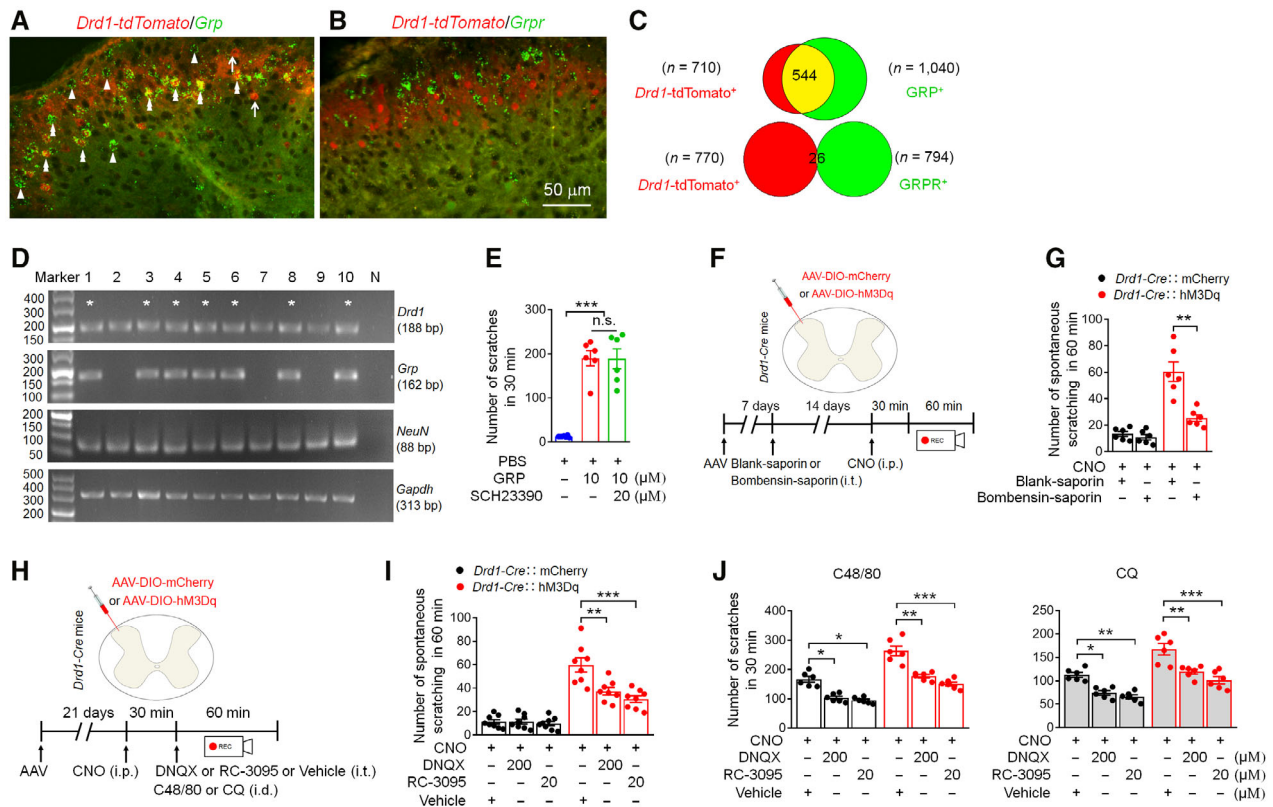


Figure 7. GRP and glutamate contribute to DRD1-mediated itch transmission.

A, B Representative images show the staining of *Grp*-probe (A) and *Grpr*-probe (B) in the SDH of *Drd1*-tdTomato mice. Arrows indicate *Drd1*-tdTomato⁺ neurons, arrowheads indicate *Grp*⁺ neurons, and double arrowheads indicate *Drd1*-tdTomato⁺*Grp*⁺ neurons. Scale bar, 50 μ m.

C Venn diagrams illustrate the co-localization percentage of DRD1⁺ neurons with GRP⁺ and GRPR⁺ neurons.

D Single-cell RT-PCR shows the expression of *Drd1*, *Grp*, *NeuN*, and *Gapdh* mRNA in tdTomato⁺ neurons. N, negative control. * Indicate *Drd1*⁺*Grp*⁺ neurons.

E Effect of SCH23390 on the scratching induced by i.t. injection of GRP. *** P < 0.001, n.s., not significant. One-way ANOVA followed by Bonferroni's test. n = 6–7 mice/group.

F Scheme of AAV injection into the SDH to express mCherry or hM3Dq in DRD1⁺ neurons in *Drd1-Cre* mice (upper panel). The timeline of the experimental setup (lower panel).

G Effect of bombensin saporin or blank saporin i.t. injection on the spontaneous scratching of mice with spinal DRD1⁺ neurons expressing mCherry or hM3Dq activated by CNO. ** P < 0.01. Student's t -test. n = 6 mice/group.

H Scheme of AAV injection into the spinal cord to express mCherry or hM3Dq in DRD1⁺ neurons of *Drd1-Cre* mice (upper panel). The timeline of the experimental setup (lower panel).

I Effect of DNQX, RC-3095, or vehicle on the spontaneous scratching of mice with spinal DRD1⁺ neurons expressing mCherry or hM3Dq and activated by CNO. ** P < 0.01, *** P < 0.001. One-way ANOVA followed by Bonferroni's test. n = 8 mice/group.

J Effect of DNQX, RC-3095, or vehicle on the scratching behaviors of mice with spinal DRD1⁺ neurons expressing mCherry or hM3Dq and activated by CNO in C48/80 model (left) or CQ model (right). * P < 0.05, ** P < 0.01, *** P < 0.001. One-way ANOVA followed by Bonferroni's test. n = 6 mice/group.

Data information: Bars represent mean values. Error bars indicate the SEM.

Source data are available online for this figure.

serotonergic and noradrenergic descending pathways in the regulation of itch processing in the SDH (Gotoh *et al.*, 2011; Zhao *et al.*, 2014a; Liu *et al.*, 2019a; Koga *et al.*, 2020). Here, using behavioral, morphological, pharmacological, electrophysiological, chemogenetic, and optogenetic approaches, we demonstrate that the dopaminergic descending projection facilitates itch transmission via DRD1⁺-GRPR⁺ neurons in the spinal cord. First, peripheral pruritogens activate dopaminergic neurons in the A11, and inhibition of dopaminergic^{A11-SDH} neurons decreases acute and chronic itch-induced scratching behaviors. Furthermore, pharmacological inhibition of DRD1 or chemogenetic inhibition of spinal DRD1⁺ neurons alleviated scratching behavior induced by acute and chronic pruritogens. Additionally, DRD1⁺ neurons are excitatory and express GRP, and a majority of DRD1⁺ neurons form a monosynaptic connection with GRPR⁺ neurons and activate these neurons via AMPA receptor. As GRPR⁺ neurons play an essential role in gating spinal itch transmission (Sun *et al.*, 2009; Liu *et al.*, 2019a), dopaminergic^{A11-SDH} neurons may facilitate spinal itch transmission via releasing glutamate and GRP to enhance the activation of GRPR⁺ neurons in the SDH. Thus, our study reveals a novel role and mechanism of descending dopaminergic pathways in itch signal processing.

The regulation of dopaminergic^{A11-SDH} neurons on spinal itch transmission

Dopaminergic neurons play an important role in diverse functions including sensory processing, motor behavior, and associative learning (Schultz, 2007). The mesolimbic dopaminergic system has been widely studied as it is involved in addiction and Parkinson's disease (Bjorklund & Dunnett, 2007). VTA dopaminergic neurons contribute to pruritogen-induced scratching behavior (Yuan *et al.*, 2018) and the reward to scratch-induced relief of itch (Su *et al.*, 2019). A11 dopaminergic neurons have long axons to the spinal dorsal horn and ventral horn and provide the only central spinal dopaminergic innervation (Skagerberg & Lindvall, 1985). Previous studies revealed the function of dopaminergic descending projection in pathological pain (Millan, 2002; Puopolo, 2019) and restless leg syndrome (Ondo *et al.*, 2000; Clemens *et al.*, 2006). In this study, fiber photometry recording showed the increase in Ca²⁺ activities of dopaminergic^{A11-SDH} neurons in response to acute or chronic itch, even with Elizabethan collars to protect the mice from scratching, indicating that the dopaminergic^{A11-SDH} neurons in the A11 are activated by the itch sensation but not by scratching-induced mechanical nociception or itch relief.

The A11 nucleus receives innervation from the limbic forebrain such as the anterior cingulate cortex (ACC), the medial and lateral hypothalamus, and brain stem nuclei including the raphe nuclei, PAG, and the parabrachial nucleus (PBN; Abrahamson & Moore, 2001). Several of these areas have been reported to be activated in functional imaging studies of itch (Darsow *et al.*, 2000; Mochizuki *et al.*, 2003; Yosipovitch *et al.*, 2008; Papoiu *et al.*, 2012; Jeong & Kang, 2015; Mochizuki & Kakigi, 2015). Moreover, neurons in the ACC, PAG, and PBN are activated by the pruritogens in mice (Mu *et al.*, 2017; Lu *et al.*, 2018; Gao *et al.*, 2019). As no evidence shows the innervation of the A11 from the spinal cord, the A11 neurons may be activated indirectly by these brain areas under itch conditions.

The A11 comprises at least three types of neurons: TH, calbindin, or both TH and calbindin (Ozawa *et al.*, 2017). Microinjection of

6-OHDA in the A11 greatly reduces TH⁺ neurons and decreases the levels of dopamine in the spinal cord (Zhao *et al.*, 2007). The 6-OHDA treatment attenuated C48/80-, CQ-, and even DCP-induced scratching behaviors. In addition, specific inhibition of dopaminergic^{A11-SDH} neurons decreased the pruritogen-evoked scratching, whereas the activation of these neurons increased the scratching behavior, indicating the facilitation of dopaminergic neurons on spinal itch transmission. However, the excitation of A11 dopaminergic neurons reduces noxious stimulation-produced responses via the activation of DRD2 in the spinal cord and spinal trigeminal nucleus caudalis (Fleetwood-Walker *et al.*, 1988; Charbit *et al.*, 2009; Taniguchi *et al.*, 2011; Liu *et al.*, 2019b), indicating a different role of the descending dopaminergic pathway on itch and pain, which is similar to the function of descending serotonergic pathway (Zhao *et al.*, 2014a). Furthermore, chemogenetic or optogenetic activation of dopaminergic^{A11-SDH} neurons did not induce spontaneous scratching. Optogenetic stimulation of VTA dopaminergic neurons does not evoke spontaneous scratching either, even though these neurons promote acute itch (Yuan *et al.*, 2018; Su *et al.*, 2019), suggesting that these dopaminergic neurons play a regulatory role in itch processing. Chemogenetic modulation of dopaminergic^{A11-SDH} neurons did not affect basal pain and locomotor function of mice, which is consistent with a recent study (Liu *et al.*, 2019b). However, Koblinger *et al.* (2018) reported that photostimulation of Chr2-transfected neurons in the A11 region enhances motor activity, which may be due to the activation of both TH⁺ and TH⁻ neurons that project to not only spinal cord but also other brain areas (Takada *et al.*, 1988; Takada, 1990, 1993). Our data showed that inhibition or activation of dopaminergic^{A11-SDH} neurons, respectively, reduced or increased c-Fos expression in the cervical spinal cord, supporting the descending modulation of A11 dopaminergic neurons on itch processing at the spinal cord level.

The role of DRD1 in acute and chronic itch

The functions of dopamine are mediated by D1-like receptors and D2-like receptors. D1-like receptors are coupled to G α s proteins which stimulate the activity of adenylyl cyclase (AC) and the production of cAMP; D2-like receptors are coupled to G α i/o proteins which inhibit the activity of AC and the production of cAMP (Missale *et al.*, 1998; Vallone *et al.*, 2000). Previous studies demonstrated that D1-like receptors and D2-like receptors, respectively, mediate pro-nociceptive and anti-nociceptive effects (Gao *et al.*, 2001; Cobacho *et al.*, 2014; Kim *et al.*, 2015; Liu *et al.*, 2019b). Systemic injection of a low dose of D1-like receptor antagonist SCH23390 reduces bombesin-induced grooming behavior but not locomotor activity, whereas D2-like receptor antagonist eticlopride inhibited both grooming and locomotion, with more inhibition on locomotion (Merali & Piggins, 1990). Systemic or intracisternal injection of SCH23390 also attenuated the C48/80- or neuromedin C-induced scratching/grooming behavior (Van Wimersma Greidanus & Maigret, 1991; Akimoto & Furuse, 2011). Our data further showed that SCH23390 reduced the scratching behavior induced by C48/80, CQ, and DCP, without effects on locomotor activity. However, sulpiride, the D2-like receptor antagonist, did not affect scratches or locomotion. In line with these data, SCH23390 decreased the c-Fos expression in the spinal cord. These data collectively indicate that D1-like receptors play a major role in spinal itch transmission.

Besides the spinal cord, dopamine receptors are also expressed in DRG neurons (Xie *et al.*, 1998; Galbavy *et al.*, 2013), and i.t. injection of inhibitors may affect receptors in both the spinal cord and DRG. Using chemogenetic approaches, we demonstrated that specific ablation or inhibition of spinal DRD1⁺ neurons attenuated scratching behaviors induced by acute or chronic pruritogens, and the activation of DRD1⁺ neurons enhanced C48/80 or CQ-evoked scratching behaviors. In addition, chemogenetic activation of DRD1⁺ neurons induced spontaneous itch-like behaviors. However, D1-like receptor agonist SKF38393 alone did not induce itch but increased the scratching induced by CQ or C48/80. Consistently, SKF38393 or optogenetic stimulation of dopaminergic^{A11-SDH} projection terminals did not induce action potential but increased electrical stimuli-induced firing frequency, indicating that activation of D1R is not sufficient to induce the activation of DRD1⁺ neurons but can enhance DRD1⁺ neuronal excitability under itch states.

Spinal DRD1⁺ neurons contribute to itch transmission via the activation of GRPR⁺ neurons

It has been demonstrated that all dopamine receptors are expressed in the spinal cord with the density and the level of expression that may change in different laminae (Puopolo, 2019). Up to now, the spatial distribution of DRD1⁺ neurons in the spinal cord is still controversial (Zhu *et al.*, 2007; Megat *et al.*, 2018). In this study, *Drd1*-tdTomato⁺ neurons were densely assembled in the laminae dlII and vII, and most of DRD1⁺ neurons were co-localized with excitatory neuronal marker vGluT2. Aira *et al.* (2016) also showed the co-localization of DRD1 with vGluT2 by immunofluorescence staining. Previous studies showed that spinal excitatory neurons play an important role in chemical itch, and several itch-related proteins including GRP, GRPR, somatostatin, and preprotachykinin 1 are all expressed in spinal excitatory neurons (Mishra & Hoon, 2013; Wang *et al.*, 2013; Gutierrez-Mecinas *et al.*, 2017; Fatima *et al.*, 2019; Pagani *et al.*, 2019).

Spinal GRP⁺ neurons form a synaptic connection with GRPR⁺ neurons to open the gate for itch (Pagani *et al.*, 2019). Here, we showed that, morphologically, spinal DRD1⁺ and GRPR⁺ neurons form synapses in the SDH. Functionally, activation of DRD1⁺ neurons induced stable EPSCs in GRPR⁺ neurons, which was blocked by AMPAR antagonist DNQX, indicating that GRPR⁺ neurons receive excitatory glutamate from DRD1⁺ neurons. In addition, the application of 4-AP reactivated the inward current in more than half of the GRPR⁺ neurons after blocking the presynaptic APs by TTX, supporting that there are monosynaptic communications between DRD1⁺ and GRPR⁺ neurons. Furthermore, chemogenetic activation of DRD1⁺ neurons-induced spontaneous itch behavior was abolished after GRPR⁺ neurons ablation and was also reduced by antagonists for glutamate and GRPR, indicating that DRD1⁺ neurons communicate with GRPR⁺ neurons via glutamate and GRP. Our results showed that 70% of DRD1⁺ neurons express GRP. Thus, although the role of spinal GRP⁺ neurons in itch transmission is controversial (Pagani *et al.*, 2019; Barry *et al.*, 2020), our data support the involvement of these neurons in itch processing. As about 30% of DRD1⁺ neurons do not express GRP, we do not exclude the regulation of DRD1⁺ on GRPR⁺ neurons via glutamate only. In addition, some DRD1⁺ neurons form polysynaptic connections with GRPR⁺ neurons, suggesting that DRD1⁺ neurons also indirectly regulate GRPR⁺ neurons via other interneurons.

In summary, our study establishes that dopaminergic^{A11-SDH} neurons are recruited in the descending regulation of spinal itch transmission. Dopaminergic^{A11-SDH} projection acts on DRD1 in excitatory interneurons, and DRD1⁺ neurons form a monosynaptic connection with GRPR⁺ neurons to modulate spinal itch transmission. Therefore, the descending A11-SDH dopaminergic projection is critical for the regulation of itch processing and could be manipulated to treat chronic itch. It is noteworthy that the present study was performed in male mice. It has been reported that female mice have fewer lumbar-projecting A11 DA neurons and lower DA concentrations in the lumbar spinal cord than male mice (Pappas *et al.*, 2008, 2010). Thus, the role of this A11 descending pathway in itch modulation in female mice needs to be investigated in the future.

Materials and Methods

Experimental animals

All adult male C57BL/6 mice were purchased from the Experimental Animal Center of Nantong University (Jiangsu, China). *Grpr-Flpo* mice were kindly gifted by Dr. Yan-Gang Sun (Chinese Academy of Sciences). *Drd1*-tdTomato mice (JAX, #016204), *Ai9* mice (JAX, #007905), *Gad67-EGFP* mice (JAX, #007673), and *TH-Cre* mice (JAX, #008601) were purchased from the Jackson laboratory. *Drd1-Cre* mice (#030778-UCD) and *Drd2-EGFP* mice (#036931-UCD) were purchased from MMRRC (Mutant Mouse Regional Resource Center). Animals were maintained in a specific pathogen-free facility under a 12:12 h light–dark cycle at a room temperature of 22 ± 2°C with food and water *ad libitum*. All animal experiments and surgeries were reviewed and approved by the Animal Care and Use Committee of Nantong University. The treatments for mice are in accordance with the guidelines of the International Association for the Study of Pain.

Spinal cord and brain stereotaxic microinjection

Mice were anesthetized with continuous inhalation of 2.0% isoflurane/1.5% oxygen mixture during the surgery. Spinal cord microinjection was performed as described by Mu *et al.* (2017). In brief, the cervical vertebral column was held by a mouse adaptor (RWD Instruments, Shenzhen, China), and then the cervical vertebral laminae were carefully removed to expose cervical segments (C4–C6). AAVs and 2% FluoroGold (FG, Fluorochrome, #52-9400) were injected unilaterally or bilaterally into the cervical spinal cord according to the design of experiments (three injection sites for one side, 200 nl of AAV or FG for each site interspaced by 400 μm). The capillary glass microelectrode was controlled by a Micro4/nanoliter infusion instrument (World Precision Instruments, USA) to deliver AAVs or FG into laminae I–II of the spinal cord at 40 nl/min (Wu *et al.*, 2021). For the A11 microinjection, mice were mounted on a small animal stereotaxic instrument with a digital display readout (RWD Instruments). The mouse scalp was incised to expose the skull surface, and then holes were bilaterally or unilaterally drilled above the A11 according to the design of experiments (the coordinate: 2.54 mm posterior to Bregma, 0.50 mm lateral to the midline, and 3.7 mm ventral to the skull surface). A volume of 200 nl AAVs or 6-OHDA (Sigma-Aldrich, #H4381) was delivered by the system of

Micro4/nanoliter infusion instrument (WPI) at a rate of 40 nl/min. After microinjection, the glass microelectrode remained in place for ~ 5 min before retraction. The muscle was closed with the Tissue Adhesive (3M Vetbond™, USA), and then the skin was sutured. AAVs were purchased from Shanghai OBiO Technology Corp Ltd and Taitool Bioscience Co. AAVs for the spinal cord and A11 microinjection were as follows: AAV-DIO-mCherry (titer 1.11×10^{13} v.g./ml), AAV-DIO-hM3Dq-mCherry (titer 1.23×10^{13} v.g./ml), AAV-DIO-hM4Di-mCherry (titer 9.95×10^{12} v.g./ml), AAV-fDIO-EGFP (titer 1.39×10^{13} v.g./ml), AAV-DIO-taCasp3-TEVp (titer 1.15×10^{13} v.g./ml), AAV-DIO-hChR2-mCherry (titer 1.09×10^{13} v.g./ml), AAV-retro-DIO-Flpo (titer 1.29×10^{13} v.g./ml), AAV-fDIO-hM3Dq-mCherry (titer 1.82×10^{13} v.g./ml), AAV-fDIO-mCherry (titer 2.13×10^{13} v.g./ml), AAV-fDIO-hM4Di-mCherry (titer 1.71×10^{13} v.g./ml), AAV-retro-Flpo (titer 1.35×10^{13} v.g./ml), AAV-fDIO-GCaMP6s (titer 2.9×10^{13} v.g./ml), AAV-fDIO-EYFP (titer 2.03×10^{13} v.g./ml), AAV-fDIO-hChR2-mCherry (titer 1.09×10^{13} v.g./ml), AAV-DIO-pre-mGRASP-P2A-mCherry (titer 1.02×10^{13} v.g./ml), and AAV-fDIO-post-mGRASP (titer 7.01×10^{12} v.g./ml).

Dopaminergic^{A11-SDH} neuron label with AAV

To target dopaminergic^{A11-SDH} neuron, we injected a Cre-dependent retro-AAV-encoding Flpo recombinase (AAV-retro-DIO-Flpo) into the cervical SDH of *TH-Cre* mice, then injected Flpo-dependent AAVs, including AAV-fDIO-GCaMP6s (expressing calcium indicator GCaMP6s), AAV-fDIO-EYFP, AAV-fDIO-mCherry, AAV-fDIO-hM4Di, AAV-fDIO-hM3Dq, or AAV-fDIO-hChR2 into the A11. In acute itch model, retro-AAV was unilaterally injected into the cervical SDH, and 1 week later, other AAVs were injected into the ipsilateral A11. In chronic itch model, these AAVs were bilaterally injected.

Fiber photometry and optogenetic stimulation

To record the activities of dopaminergic^{A11-SDH} neurons during scratching, optical fibers (1.25 mm O.D., 200 μm fiber core, and NA = 0.37, 3.5 mm long) were implanted into the A11 at about 200 μm above the AAV-injected dopaminergic^{A11-SDH} neuron population. Optical fibers (Inper, Hangzhou, China) were fixed to the skull with super glue and dental cement. After surgery, mice were allowed to recover for 10 days before experiments. The fixed optical fibers were gently held and connected to the fiber photometry system (QAXK-FPS-LED, ThinkerTech, Nanjing, China) through a fiber optic rotary joint (QAXK-HP). For fiber photometry, the laser power of 470 nm at the tip of the optical fiber was adjusted to 50 μW to avoid bleaching the GCaMP6s proteins. A video was recorded to synchronize the timeline of GCaMP6s fluorescent signals and scratching behaviors. To prevent scratching the nape skin, an Elizabethan collar (EC201V, Kent Scientific Corporation, USA) was used. To observe the effect of hind paw movement on GCaMP6s fluorescent signals, a 3 mm × 1 mm sticky tape was adhered to the ear of mice. The recorded GCaMP6s fluorescent signals were transferred to a MATLAB mat file and analyzed by a custom-written MATLAB code. Data were matched to scratching behaviors based on individual trials. Fluorescence change was shown as $\Delta F/F$, which was measured by $(F - F_0)/F_0$. The F and F_0 values represent the fluorescent value at each time point and the average of fluorescent values during the baseline period, respectively. To quantify the

fluorescent change between the baseline and scratching train onset periods, the $\Delta F/F$ values from -2 to -1 s and 3 to 5 s relative to the scratching train onset were averaged as baseline and onset values, respectively.

For optogenetic stimulation *in vivo*, a 473 nm laser power source (Aurora-220, Newdoom, China) was connected to the optical fiber fixed on the mouse skull, and the laser power at the tip of the optical fiber was adjusted to 6 mW/cm². In the process of the experiment, 473 nm blue light was delivered in 10 ms pulses at 20 Hz with five cycles of 3 min light-on and 3 min light-off (Su *et al*, 2019). The scratching behaviors during blue light stimulation were recorded.

Drug delivery

For intrathecal administration, SCH23390 (Sigma-Aldrich, #D054), Sulpiride (Sigma-Aldrich, #S8010), SKF38393 (Sigma-Aldrich, #S101), GRP (Tocris Bioscience, #1789), DNQX (Sigma-Aldrich, #D0540), and RC-3095 (Sigma-Aldrich, #R9653) were injected by a 30 G needle into the cerebrospinal fluid between the fourth and fifth lumbar vertebral arches. For ablation of GRPR⁺ neurons in the spinal cord, mice were intrathecally administered bombesin saporin (400 ng, Advanced Targeting Systems, #IT-40) or blank saporin (400 ng, Advanced Targeting Systems, #IT-21) 2 weeks before behavioral tests. For pharmacogenetics manipulation, mice were intraperitoneally injected with clozapine-N-oxide (CNO, 1 mg/kg, 100 μl, Enzo Life Sciences, #BML-NS105). After 30 min, the behavioral tests were conducted on the mice.

Behavioral tests

Mice were placed into the testing apparatus daily for at least 3 days before behavioral tests. The temperature of the behavioral testing room was kept at $22 \pm 2^\circ\text{C}$ with 50 ~ 60% ambient humidity. All investigators executing behavioral tests were blinded to treatments.

Acute itch

Mice were daily placed into the testing apparatus until they became quiet before the itch behavioral tests. The nape skin was shaved 2 days before the experiments. On the day of the itch behavioral tests, mice were individually placed in small plastic apparatus on an elevated metal mesh floor and allowed at least 30 min for habituation. Under brief anesthesia with isoflurane, mice were given an intradermal injection of 50 μl of compound 48/80 (C48/80; Sigma-Aldrich, #C2313) or chloroquine (CQ; Sigma-Aldrich, #C6628) via a 30G needle into nape skin. Immediately after the injection, mice were returned to their chambers and recorded for 30 min. The video recording was subsequently played back offline and the scratching behavior was quantified in a blinded manner. A bout of scratching was counted when a mouse lifted the hind paw to scratch the shaved nape skin and returned the hind paw to the floor or the mouth (Han *et al*, 2018).

Diphenylcyclopropenone (DCP)-induced chronic itch in the nape skin

The skin of nape was shaved in an area of approximately 1.0 × 1.0 cm 1 day before establishing the DCP model. DCP (Shanghai Aladdin Biochem Technology Co., Ltd) was resolved to 1% in acetone and topically painted (0.2 ml) to the shaved skin of nape.

Seven days later, the mice were challenged by painting the nape skin with 0.5% DCP (0.2 ml; Liu *et al*, 2016), which was applied daily for 6–8 days. Mice were habituated to the transparent boxes (10 × 10 × 18 cm) on an elevated metal mesh floor for at least 3 days before the itch behavioral tests. The spontaneous scratching behavior was video recorded for 60 min after each 0.5% DCP application. Bouts of scratching were then counted in a blinded manner (Zhang *et al*, 2018).

Mechanical itch

Mice were habituated in the apparatus with a mesh cover. Von Frey filaments (0.008, 0.04, and 0.07 g) were vertically delivered to the shaved nape skin. The movement of hind paw toward mechanical-stimulated nape skin was noted as a positive scratch response. Each von Frey filament was delivered five times at a 2-min interval on the ipsilateral nape skin. Response percentages were calculated to evaluate the degree of mechanical itch.

Mechanosensation and thermosensation tests

As hind paws were used to check pain sensitivity, we injected AAV-retro-DIO-Flpo into the bilateral lumbar SDH of *TH-Cre* mice (Zhang *et al*, 2016), then injected Flpo-dependent AAVs into the A11. For the mechanosensation test, mice were placed into boxes on an elevated mesh floor. The plantar surface of the ipsilateral hind paw was vertically delivered with a series of von Frey filaments ranging from 0.02 to 2.0 g. The 50% paw withdrawal threshold was calculated using Dixon's up-down method (Chaplan *et al*, 1994). For thermosensation tests, Hargreaves and hot/cold plate tests were used. For Hargreaves test, mice were placed into plastic boxes on a glass plate. The ipsilateral plantar surface of hind paw was heated by a beam of radiant energy (IITC Life Science, USA). The latencies to hind paw withdrawal were recorded. The cutoff time was set at 20 s to prevent hind paw injury (Hargreaves *et al*, 1988). For the hot/cold plate test, mice were placed into plastic boxes on a hot/cold plate (IITC Life Science). The plate surface temperature was set at 50, 52, 54, or 0°C, and the latencies to hind paw flinching and licking were recorded. The cutoff time was correspondingly set at 60, 50, 30, or 20 s to avoid hind paw injury. Each mouse was tested three times at 10 min intervals.

Rotarod test

The mouse motor function was examined by the Rotarod equipment (IITC Life Science). Before testing, mice were trained on the rotarod rotating at a constant speed of 10 rpm for 3 min every day, until the day the mice no longer fell off the rotarod. For testing, the speed of rotation was set at a speed of 10 rpm for 1 min and subsequently accelerated to 80 rpm in 5 min. We recorded the latency to fall since the beginning of the acceleration as an estimation for the motor function. The latency was averaged over three trials, separated by a 10-min interval (Zhang *et al*, 2018).

Open-field locomotion test

For the locomotor function test, mice were habituated in a light-gray chamber (50 cm × 50 cm × 40 cm) for 15 min per day and 3 days before testing. For testing, mice in the open field were recorded for 5 min, and the travel distance was automatically analyzed using smart software (VisuTrack 3.0.0.1, Shanghai XinRuan Information Technology Co., Ltd., Shanghai, China).

Real-time quantitative RT-PCR (qPCR)

The total RNA of the spinal cord was collected according to the protocol of TRIzol reagent (Invitrogen, USA). The quantity and quality of total RNA were checked on a NanoDrop spectrophotometer (ThermoScientific). The cDNA was synthesized from RNA by using Reverse Transcription System (Promega GoScript™, USA) according to the manufacturer's instructions. The qPCR analysis was run on the A&B Applied Biosystems platform with SYBR Premix Ex Taq II kit (Takara, #RR820A). The following primers were used in the real-time PCR reaction: *Drd1* forward: 5'-GAC ACG AGG TTG AGC AGG ACA TAC-3', *Drd1* reverse: 5'-GTG GTG GTC TGG CAG TTC TTG G-3'; *Gapdh* forward: 5'-AAA TGG TGA AGG TCG GTG TGA AC-3', *Gapdh* reverse: 5'-CAA CAA TCT CCA CTT TGC CAC TG-3'. PCR amplification was set at 95°C for 30 s, followed by 40 cycles of 5 s for 95°C and 30 s for 60°C. PCR data were displayed with StopOne Software v2.3. Melting curves were performed to ensure that the nonspecificity of PCR products was absent. $2^{-\Delta\Delta C_t}$ method was used to analyze the data that were quantified by normalizing the *Drd1* cycle threshold (C_t) values with *Gapdh* C_t .

Immunofluorescence staining

Animals were deeply anesthetized with isoflurane and perfused through the ascending aorta with 0.01 M PBS followed by 4% paraformaldehyde in 0.01 M PB. After the perfusion, the spinal cord and brain were collected, postfixed in paraformaldehyde for 2 h, and dehydrated in 30% sucrose at 4°C. For immunofluorescence staining, the spinal cord and brain were cut into 30 μm free-floating sections in a cryostat (Leica CM 1950, Germany) as we described previously (Zhang *et al*, 2018). One section was picked up to stain for immunofluorescence qualification at every four sections. The sections were first blocked with 5% donkey serum for 2 h at RT (room temperature), then incubated with the following primary antibodies overnight at 4°C: c-Fos (guinea pig, Synaptic Systems, #226004), NK1R (goat, Santa Cruz, #sc-14115), CGRP (mouse, Sigma-Aldrich, #C7113), PKCγ (rabbit, Santa Cruz, #sc-211), PAX2 (rabbit, ThermoFisher, #71-6000), NeuN (rabbit, Abcam, #ab177487), and TH (rabbit, Millipore, #AB152). The sections were then incubated for 2 h at RT with FITC or Cy3-conjugated secondary antibodies (1:1,000, Jackson ImmunoResearch) or IB4-FITC (Sigma-Aldrich, #L2895). The stained sections were checked with a Nikon Eclipse Ni-E fluorescence microscope, and images were captured with a CCD Spot camera. Three stained sections from one mouse were used for quantification, which was conducted in a blinded manner.

Fluorescence in situ hybridization (FISH)

The collection procedure for the spinal cord is the same as immunofluorescence staining. The 12-μm-thick frozen sections of the spinal cord were mounted onto Superfrost Plus slides (FisherScientific, USA). The probes directed against mouse *Drd1* (#461901), *slc17a6* (#319171), *Grp* (#317861), and *Grpr* (#317871) were designed by Advanced Cell Diagnostics. The FISH for these probes was performed according to the RNAscope system described in the Multiplex Fluorescence Kit v2 (Advanced Cell Diagnostics, #323100). In some cases, sections were counterstained with DAPI (Life Technologies) to show cell nuclei.

Single-cell RT-PCR

The processing procedure of spinal cord slices from *Drd1-tdTomato* mice is the same as the preparation for slice electrophysiology. The single-cell RT-PCR protocol was performed as we previously described (Zhang *et al.*, 2018). Briefly, tdTomato⁺ neurons in spinal slices were inhaled into an RNAase-free glass pipette with a tip diameter of ~ 20 μm, and then carefully pushed into a tube containing the reverse transcription reagents. The first step of the reaction was performed to remove the genomic DNA (Invitrogen; #AM2235) at the condition of 37°C for 40 min and then 80°C for 10 min. The second step of the reaction was reversely transcribed from RNA to cDNA by using the Reverse Transcription System (Invitrogen; #18080-051) at the condition of 50°C for 50 min and 70°C for 15 min. The harvested cDNA was then used in a two-round PCR (Takara, #RR820A). The first round of PCR was performed in 10 μl of PCR buffer containing “outer” primers of *Drd1*, *Grp*, *NeuN*, and *Gapdh*, respectively. The amplification of the first round of PCR was set at 95°C for 5 min, followed by 30 cycles of 40 s for 95°C, 40 s for 58°C, 40 s for 72°C, and then completed at 72°C for 7 min of final elongation. The DNA products of the first-round PCR were diluted 1,000-fold to amplify in the second round of PCR, which contained 10 μl of PCR buffer with the corresponding “inner” primers. The amplification condition was the same as the first round of PCR. The RT-PCR procedure for the negative control is the same as above, except there is no neural tissue in the collecting bath solution. The final PCR products were visualized and identified by GelRed[®] fluorescent nucleic acid dye (Biotium, #41003) in 3% agarose gels. The sequences of single-cell PCR primers are listed in Appendix Table S2.

Electrophysiological slice recording

The spinal cord and brain were quickly removed from the transgenic mice under deep anesthesia using isoflurane and then immersed in an ice-cold slicing solution with continuously oxygenated in 95% O₂ plus 5% CO₂. The slicing solution contains (in mM): 235 sucrose, 25 NaHCO₃, 3 KCl, 1.25 NaH₂PO₄, 1 CaCl₂, 2.5 MgCl₂, and 10 glucose. Coronal cervical spinal cord slices (400 μm thick) and brain slices (300 μm thick) were cut with a vibratome (VT1000S; Leica). Slices were transferred into oxygenated (95% O₂ + 5% CO₂) artificial cerebrospinal fluid (aCSF) containing (in mM): 125 NaCl, 3 KCl, 1.2 NaH₂PO₄, 2.5 CaCl₂, 1.2 MgCl₂, 25 NaHCO₃ and 25 glucose at 34°C for 30 min, and then recovered at room temperature for 1.5 h before recording. Following recovery, the slices were transferred to a recording chamber and continuously perfused with oxygenated aCSF at a rate of 1 ~ 2 ml/min. The intracellular solution contains the following (in mM): 120 K-gluconate, 10 HEPES, 20 KCl, 0.2 EGTA, 2 MgCl₂, 0.3 GTP-Tris, and 4 Na₂ATP, pH 7.2 ~ 7.4 (adjusted by KOH). Fluorescence-marked (tdTomato or mCherry-labeled) neurons in the SDH or the A11 were visualized using a microscope (BX51WI, Olympus, Japan) with epifluorescence, CMOS camera, and a high-power LED fluorescence light source (Lambda HPX-L5, Sutter Instrument). Whole-cell patch-clamp recordings on fluorescence-labeled neurons were conducted using an amplifier (Multiclamp 700B; Molecular Devices) and digitizer (DigiData 1440A; Molecular Devices). Signals were digitized at 10 kHz and low-pass filtered at 2 kHz. Membrane input resistance

was continuously monitored by using a current pulse of –10 pA following each test. Data were discarded when the series resistance changed > 20% from their original state during the recording. After establishing the whole-cell configuration, a series of 1 s duration depolarizing current pulses (0–100 pA, +10 pA/step) were injected into the cell to evoke action potentials. After a stable current-clamp recording (baseline), 10 μM CNO was added into the aCSF to continuously perfuse the spinal or brain slice for 5 min to test the effectiveness of hM4Di and hM3Dq expressed in DRD1⁺ or dopaminergic neurons. To check the effect of dopaminergic^{A11-SDH} neurons on the activity of spinal DRD1⁺ neurons, current-clamp recordings combining with optogenetics were performed in spinal slices prepared from mice expressing hChR2 in dopaminergic^{A11-SDH} neurons and tdTomato in spinal DRD1⁺ neurons. The laser power at the tip of the optic fiber was 2 ~ 3 mW/cm², and the bursting stimulation contained five pulses at 20 Hz that was repeated every 1,000 ms. To determine the type of synaptic connection from spinal DRD1⁺ neurons to GRPR⁺ neurons, voltage-clamp recordings combining with optogenetic methods were performed in spinal slices prepared from mice expressing hChR2 in DRD1⁺ neurons and EGFP in GRPR⁺ neurons. DRD1⁺ neurons or terminals of dopaminergic^{A11-SDH} neurons were irradiated with light (470 nm, 2 ms) emitted from an LED plate.

Statistical analysis

All data were presented as mean ± SEM and analyzed using GraphPad Prism 8.0.1 software. The sample size of each experiment was provided in the Results. Statistical analysis of two experimental groups was performed using a two-tailed Student's *t*-test. Comparisons of more than two groups were performed using one-way ANOVA or two-way repeated-measures (RM) ANOVA followed by post-hoc Bonferroni's test. The criterion for statistical significance was *P* < 0.05.

Data availability

The datasets generated during this study are available from the corresponding authors upon reasonable request. This study includes no data deposited in external repositories.

Expanded View for this article is available [online](#).

Acknowledgements

The project was supported by the National Natural Science Foundation of China (32030048; 31970938; 82271256), The Natural Science Foundation of Jiangsu Province, China (BK20191448).

Author contributions

Zhi-Jun Zhang: Conceptualization; data curation; funding acquisition; investigation; writing – original draft. **Han-Yu Shao:** Investigation. **Chuan Liu:** Investigation. **Hao-Lin Song:** Investigation. **Xiao-Bo Wu:** Investigation. **De-Li Cao:** Investigation. **Meixuan Zhu:** Investigation. **Yuan-Yuan Fu:** Investigation. **Juan Wang:** Investigation. **Yong-Jing Gao:** Conceptualization; supervision; funding acquisition; writing – original draft; writing – review and editing.

Disclosure and competing interest statement

The authors declare that they have no conflict of interest.

References

- Abrahamson EE, Moore RY (2001) The posterior hypothalamic area: chemoarchitecture and afferent connections. *Brain Res* 889: 1–22
- Aira Z, Barrenetxea T, Buesa I, Garcia Del Cano G, Azkue JJ (2016) Dopamine D1-like receptors regulate constitutive, μ -opioid receptor-mediated repression of use-dependent synaptic plasticity in dorsal horn neurons: more harm than good? *J Neurosci* 36: 5661–5673
- Akimoto Y, Furuse M (2011) SCH23390, a dopamine D1 receptor antagonist, suppressed scratching behavior induced by compound 48/80 in mice. *Eur J Pharmacol* 670: 162–167
- Albisetti GW, Pagani M, Platonova E, Hosli L, Johannssen HC, Fritschy JM, Wildner H, Zeilhofer HU (2019) Dorsal horn gastrin-releasing peptide expressing neurons transmit spinal itch but not pain signals. *J Neurosci* 39: 2238–2250
- Barry DM, Liu XT, Liu B, Liu XY, Gao F, Zeng X, Liu J, Yang Q, Wilhelm S, Yin J et al (2020) Exploration of sensory and spinal neurons expressing gastrin-releasing peptide in itch and pain related behaviors. *Nat Commun* 11: 1397
- Beaulieu JM, Gainetdinov RR (2011) The physiology, signaling, and pharmacology of dopamine receptors. *Pharmacol Rev* 63: 182–217
- Bjorklund A, Dunnett SB (2007) Dopamine neuron systems in the brain: an update. *Trends Neurosci* 30: 194–202
- Carta I, Chen CH, Schott AL, Dorizan S, Khodakhah K (2019) Cerebellar modulation of the reward circuitry and social behavior. *Science* 363: eaav0581
- Chaplan SR, Bach FW, Pogrel JW, Chung JM, Yaksh TL (1994) Quantitative assessment of tactile allodynia in the rat paw. *J Neurosci Methods* 53: 55–63
- Charbit AR, Akerman S, Holland PR, Goadsby PJ (2009) Neurons of the dopaminergic/calcatonin gene-related peptide A11 cell group modulate neuronal firing in the trigeminocervical complex: an electrophysiological and immunohistochemical study. *J Neurosci* 29: 12532–12541
- Choi JH, Sim SE, Kim JI, Choi DI, Oh J, Ye S, Lee J, Kim T, Ko HG, Lim CS et al (2018) Interregional synaptic maps among engram cells underlie memory formation. *Science* 360: 430–435
- Clemens S, Rye D, Hochman S (2006) Restless legs syndrome: revisiting the dopamine hypothesis from the spinal cord perspective. *Neurology* 67: 125–130
- Cobacho N, de la Calle JL, Paino CL (2014) Dopaminergic modulation of neuropathic pain: analgesia in rats by a D2-type receptor agonist. *Brain Res Bull* 106: 62–71
- Darsow U, Drzezga A, Frisch M, Munz F, Weilke F, Bartenstein P, Schwaiger M, Ring J (2000) Processing of histamine-induced itch in the human cerebral cortex: a correlation analysis with dermal reactions. *J Invest Dermatol* 115: 1029–1033
- Dong X, Dong X (2018) Peripheral and central mechanisms of itch. *Neuron* 98: 482–494
- Duan B, Cheng L, Ma Q (2018) Spinal circuits transmitting mechanical pain and itch. *Neurosci Bull* 34: 186–193
- Fatima M, Ren X, Pan H, Slade HFE, Asmar AJ, Xiong CM, Shi A, Xiong AE, Wang L, Duan B (2019) Spinal somatostatin-positive interneurons transmit chemical itch. *Pain* 160: 1166–1174
- Fleetwood-Walker SM, Hope PJ, Mitchell R (1988) Antinociceptive actions of descending dopaminergic tracts on cat and rat dorsal horn somatosensory neurones. *J Physiol* 399: 335–348
- Galbavy W, Safaie E, Rebecchi MJ, Puopolo M (2013) Inhibition of tetrodotoxin-resistant sodium current in dorsal root ganglia neurons mediated by D1/D5 dopamine receptors. *Mol Pain* 9: 60
- Gao X, Zhang Y, Wu G (2001) Effects of dopaminergic agents on carrageenan hyperalgesia after intrathecal administration to rats. *Eur J Pharmacol* 418: 73–77
- Gao ZR, Chen WZ, Liu MZ, Chen XJ, Wan L, Zhang XY, Yuan L, Lin JK, Wang M, Zhou L et al (2019) Tac1-expressing neurons in the periaqueductal gray facilitate the itch-scratching cycle via descending regulation. *Neuron* 101: 45–59.e9
- Gotoh Y, Andoh T, Kuraishi Y (2011) Noradrenergic regulation of itch transmission in the spinal cord mediated by alpha-adrenoceptors. *Neuropharmacology* 61: 825–831
- Gutierrez-Mecinas M, Bell AM, Marin A, Taylor R, Boyle KA, Furuta T, Watanabe M, Polgar E, Todd AJ (2017) Preprotachykinin A is expressed by a distinct population of excitatory neurons in the mouse superficial spinal dorsal horn including cells that respond to noxious and pruritic stimuli. *Pain* 158: 440–456
- Han Q, Liu D, Convertino M, Wang Z, Jiang C, Kim YH, Luo X, Zhang X, Nackley A, Dokholyan NV et al (2018) miRNA-711 binds and activates TRPA1 extracellularly to evoke acute and chronic pruritus. *Neuron* 99: 449–463.e6
- Hargreaves K, Dubner R, Brown F, Flores C, Joris J (1988) A new and sensitive method for measuring thermal nociception in cutaneous hyperalgesia. *Pain* 32: 77–88
- Hu H (2016) Reward and aversion. *Annu Rev Neurosci* 39: 297–324
- Huang J, Polgar E, Solinski HJ, Mishra SK, Tseng PY, Iwagaki N, Boyle KA, Dickie AC, Kriegbaum MC, Wildner H et al (2018) Circuit dissection of the role of somatostatin in itch and pain. *Nat Neurosci* 21: 707–716
- Ikoma A, Steinhoff M, Stander S, Yosipovitch G, Schmelz M (2006) The neurobiology of itch. *Nat Rev Neurosci* 7: 535–547
- Janssen LK, Sescousse G, Hashemi MM, Timmer MH, ter Huurne NP, Geurts DE, Cools R (2015) Abnormal modulation of reward versus punishment learning by a dopamine D2-receptor antagonist in pathological gamblers. *Psychopharmacology (Berl)* 232: 3345–3353
- Jeong KY, Kang JH (2015) Investigation of the pruritus-induced functional activity in the rat brain using manganese-enhanced MRI. *J Magn Reson Imaging* 42: 709–716
- Kardon AP, Polgar E, Hachisuka J, Snyder LM, Cameron D, Savage S, Cai X, Karnup S, Fan CR, Hemenway GM et al (2014) Dynorphin acts as a neuromodulator to inhibit itch in the dorsal horn of the spinal cord. *Neuron* 82: 573–586
- Kim J, Zhao T, Petralia RS, Yu Y, Peng H, Myers E, Magee JC (2011) mGRASP enables mapping mammalian synaptic connectivity with light microscopy. *Nat Methods* 9: 96–102
- Kim JY, Tillu DV, Quinn TL, Mejia GL, Shy A, Asiedu MN, Murad E, Schumann AP, Totsch SK, Sorge RE et al (2015) Spinal dopaminergic projections control the transition to pathological pain plasticity via a D1/D5-mediated mechanism. *J Neurosci* 35: 6307–6317
- Koblinger K, Fuzesi T, Ejdrygiewicz J, Krajacic A, Bains JS, Whelan PJ (2014) Characterization of A11 neurons projecting to the spinal cord of mice. *PLoS One* 9: e109636
- Koblinger K, Jean-Xavier C, Sharma S, Fuzesi T, Young L, Eaton SEA, Kwok CHT, Bains JS, Whelan PJ (2018) Optogenetic activation of A11 region increases motor activity. *Front Neural Circuits* 12: 86
- Koch SC, Acton D, Goulding M (2018) Spinal circuits for touch, pain, and itch. *Annu Rev Physiol* 80: 189–217
- Koga K, Shiraishi Y, Yamagata R, Tozaki-Saitoh H, Shiratori-Hayashi M, Tsuda M (2020) Intrinsic braking role of descending locus coeruleus noradrenergic neurons in acute and chronic itch in mice. *Mol Brain* 13: 144

- Liang TY, Zhou H, Sun YG (2022) Distinct roles of dopamine receptor subtypes in the nucleus accumbens during itch signal processing. *J Neurosci* 42: 8842–8854
- Liu Q, Tang Z, Surdenikova L, Kim S, Patel KN, Kim A, Ru F, Guan Y, Weng HJ, Geng Y et al (2009) Sensory neuron-specific GPCR Mrgprs are itch receptors mediating chloroquine-induced pruritus. *Cell* 139: 1353–1365
- Liu T, Han Q, Chen G, Huang Y, Zhao LX, Berta T, Gao YJ, Ji RR (2016) Toll-like receptor 4 contributes to chronic itch, allodynia, and spinal astrocyte activation in male mice. *Pain* 157: 806–817
- Liu MZ, Chen XJ, Liang TY, Li Q, Wang M, Zhang XY, Li YZ, Sun Q, Sun YG (2019a) Synaptic control of spinal GRPR(+) neurons by local and long-range inhibitory inputs. *Proc Natl Acad Sci USA* 116: 27011–27017
- Liu S, Tang Y, Shu H, Tatum D, Bai Q, Crawford J, Xing Y, Lobo MK, Bellinger L, Kramer P et al (2019b) Dopamine receptor D2, but not D1, mediates descending dopaminergic pathway-produced analgesic effect in a trigeminal neuropathic pain mouse model. *Pain* 160: 334–344
- Liu YC, Wang YJ, Lu B, Chen M, Zheng P, Liu JG (2018) ACC to dorsal medial striatum inputs modulate histaminergic itch sensation. *J Neurosci* 38: 3823–3839
- Luo SX, Huang EJ (2016) Dopaminergic neurons and brain reward pathways: from neurogenesis to circuit assembly. *Am J Pathol* 186: 478–488
- Mack MR, Kim BS (2018) The itch-scratch cycle: a neuroimmune perspective. *Trends Immunol* 39: 980–991
- Megat S, Shiers S, Moy JK, Barragan-Iglesias P, Pradhan G, Seal RP, Dussor G, Price TJ (2018) A critical role for dopamine D5 receptors in pain chronicity in male mice. *J Neurosci* 38: 379–397
- Meng QT, Liu XY, Liu XT, Liu J, Munanairi A, Barry DM, Liu B, Jin H, Sun Y, Yang Q et al (2021) BNP facilitates NMB-encoded histaminergic itch via NPRC-NMBR crosstalk. *Elife* 10: e71689
- Merali Z, Piggins H (1990) Effects of dopamine D1 and D2 receptor agonists and antagonists on bombesin-induced behaviors. *Eur J Pharmacol* 191: 281–293
- Millan MJ (2002) Descending control of pain. *Prog Neurobiol* 66: 355–474
- Mishra SK, Hoon MA (2013) The cells and circuitry for itch responses in mice. *Science* 340: 968–971
- Missale C, Nash SR, Robinson SW, Jaber M, Caron MG (1998) Dopamine receptors: from structure to function. *Physiol Rev* 78: 189–225
- Mochizuki H, Kakigi R (2015) Central mechanisms of itch. *Clin Neurophysiol* 126: 1650–1660
- Mochizuki H, Tashiro M, Kano M, Sakurada Y, Itoh M, Yanai K (2003) Imaging of central itch modulation in the human brain using positron emission tomography. *Pain* 105: 339–346
- Mu D, Deng J, Liu KF, Wu ZY, Shi YF, Guo WM, Mao QQ, Liu XJ, Li H, Sun YG (2017) A central neural circuit for itch sensation. *Science* 357: 695–699
- Ondo WG, He Y, Rajasekaran S, Le WD (2000) Clinical correlates of 6-hydroxydopamine injections into A11 dopaminergic neurons in rats: a possible model for restless legs syndrome. *Mov Disord* 15: 154–158
- Ozawa H, Yamaguchi T, Hamaguchi S, Yamaguchi S, Ueda S (2017) Three types of A11 neurons project to the rat spinal cord. *Neurochem Res* 42: 2142–2153
- Pagani M, Albiseti GW, Sivakumar N, Wildner H, Santello M, Johannssen HC, Zeilhofer HU (2019) How gastrin-releasing peptide opens the spinal gate for itch. *Neuron* 103: 102–117.e5
- Papoiu AD, Coghill RC, Kraft RA, Wang H, Yosipovitch G (2012) A tale of two itches. Common features and notable differences in brain activation evoked by cowhage and histamine induced itch. *Neuroimage* 59: 3611–3623
- Pappas SS, Behrouz B, Janis KL, Goudreau JL, Lookingland KJ (2008) Lack of D2 receptor mediated regulation of dopamine synthesis in A11 diencephalospinal neurons in male and female mice. *Brain Res* 1214: 1–10
- Pappas SS, Tiernan CT, Behrouz B, Jordan CL, Breedlove SM, Goudreau JL, Lookingland KJ (2010) Neonatal androgen-dependent sex differences in lumbar spinal cord dopamine concentrations and the number of A11 diencephalospinal dopamine neurons. *J Comp Neurol* 518: 2423–2436
- Puopolo M (2019) The hypothalamic-spinal dopaminergic system: a target for pain modulation. *Neural Regen Res* 14: 925–930
- Qu S, Ondo WG, Zhang X, Xie WJ, Pan TH, Le WD (2006) Projections of diencephalic dopamine neurons into the spinal cord in mice. *Exp Brain Res* 168: 152–156
- Schultz W (2007) Multiple dopamine functions at different time courses. *Annu Rev Neurosci* 30: 259–288
- Skagerberg G, Lindvall O (1985) Organization of diencephalic dopamine neurons projecting to the spinal cord in the rat. *Brain Res* 342: 340–351
- Su XY, Chen M, Yuan Y, Li Y, Guo SS, Luo HQ, Huang C, Sun W, Li Y, Zhu MX et al (2019) Central processing of itch in the midbrain reward center. *Neuron* 102: e855
- Sun YG, Chen ZF (2007) A gastrin-releasing peptide receptor mediates the itch sensation in the spinal cord. *Nature* 448: 700–703
- Sun YG, Zhao ZQ, Meng XL, Yin J, Liu XY, Chen ZF (2009) Cellular basis of itch sensation. *Science* 325: 1531–1534
- Takada M (1990) The A11 catecholamine cell group: another origin of the dopaminergic innervation of the amygdala. *Neurosci Lett* 118: 132–135
- Takada M (1993) Widespread dopaminergic projections of the subparafascicular thalamic nucleus in the rat. *Brain Res Bull* 32: 301–309
- Takada M, Li ZK, Hattori T (1988) Single thalamic dopaminergic neurons project to both the neocortex and spinal cord. *Brain Res* 455: 346–352
- Taniguchi W, Nakatsuka T, Miyazaki N, Yamada H, Takeda D, Fujita T, Kumamoto E, Yoshida M (2011) *In vivo* patch-clamp analysis of dopaminergic antinociceptive actions on substantia gelatinosa neurons in the spinal cord. *Pain* 152: 95–105
- Tao YM, Yu C, Wang WS, Hou YY, Xu XJ, Chi ZQ, Ding YQ, Wang YJ, Liu JG (2017) Heteromers of mu opioid and dopamine D1 receptors modulate opioid-induced locomotor sensitization in a dopamine-independent manner. *Br J Pharmacol* 174: 2842–2861
- Vallone D, Picetti R, Borrelli E (2000) Structure and function of dopamine receptors. *Neurosci Biobehav Rev* 24: 125–132
- Van Wimersma Greidanus TB, Maigret C (1991) Neuromedin-induced excessive grooming/scratching behavior is suppressed by naloxone, neurotensin and a dopamine D1 receptor antagonist. *Eur J Pharmacol* 209: 57–61
- Wang X, Zhang J, Eberhart D, Urban R, Meda K, Solorzano C, Yamanaka H, Rice D, Basbaum AI (2013) Excitatory superficial dorsal horn interneurons are functionally heterogeneous and required for the full behavioral expression of pain and itch. *Neuron* 78: 312–324
- Wu ZH, Shao HY, Fu YY, Wu XB, Cao DL, Yan SX, Sha WL, Gao YJ, Zhang JZ (2021) Descending modulation of spinal itch transmission by primary somatosensory cortex. *Neurosci Bull* 37: 1345–1350
- Xie GX, Jones K, Peroutka SJ, Palmer PP (1998) Detection of mRNAs and alternatively spliced transcripts of dopamine receptors in rat peripheral sensory and sympathetic ganglia. *Brain Res* 785: 129–135
- Yosipovitch G, Ishiiji Y, Patel TS, Hicks MI, Oshiro Y, Kraft RA, Winnicki E, Coghill RC (2008) The brain processing of scratching. *J Invest Dermatol* 128: 1806–1811
- Yuan L, Liang TY, Deng J, Sun YG (2018) Dynamics and functional role of dopaminergic neurons in the ventral tegmental area during itch processing. *J Neurosci* 38: 9856–9869
- Zhang Z-J, Jing P-B, Gao Y-J (2016) Microinjection of virus into lumbar enlargement of spinal dorsal horn in mice. *Bio Protoc* 6: e2020

- Zhang ZJ, Guo JS, Li SS, Wu XB, Cao DL, Jiang BC, Jing PB, Bai XQ, Li CH, Wu ZH et al (2018) TLR8 and its endogenous ligand miR-21 contribute to neuropathic pain in murine DRG. *J Exp Med* 215: 3019–3037
- Zhao H, Zhu W, Pan T, Xie W, Zhang A, Ondo WG, Le W (2007) Spinal cord dopamine receptor expression and function in mice with 6-OHDA lesion of the A11 nucleus and dietary iron deprivation. *J Neurosci Res* 85: 1065–1076
- Zhao ZQ, Liu XY, Jeffrey J, Karunaratne WK, Li JL, Munanairi A, Zhou XY, Li H, Sun YG, Wan L et al (2014a) Descending control of itch transmission by the serotonergic system via 5-HT1A-facilitated GRP-GRPR signaling. *Neuron* 84: 821–834
- Zhao ZQ, Wan L, Liu XY, Huo FQ, Li H, Barry DM, Krieger S, Kim S, Liu ZC, Xu J et al (2014b) Cross-inhibition of NMBR and GRPR signaling maintains normal histaminergic itch transmission. *J Neurosci* 34: 12402–12414
- Zhu H, Clemens S, Sawchuk M, Hochman S (2007) Expression and distribution of all dopamine receptor subtypes (D(1)-D(5)) in the mouse lumbar spinal cord: a real-time polymerase chain reaction and non-autoradiographic *in situ* hybridization study. *Neuroscience* 149: 885–897